SANDIA REPORT
SAND2014-0779
Unlimited Release
Printed January 2014

Evaluation of Select Heat and Pressure Measurement Gauges for Potential Use in the NRC/OECD High Energy Arc Fault (HEAF) Test Program

Carlos Lopez, William B. Wente, and Victor G. Figueroa

Prepared by
Sandia National Laboratories
Albuquerque, New Mexico 87185 and Livermore, California 94550

Sandia National Laboratories is a multi-program laboratory managed and operated by Sandia Corporation, a wholly owned subsidiary of Lockheed Martin Corporation, for the U.S. Department of Energy's National Nuclear Security Administration under contract DE-AC04-94AL85000.

Sandia National Laboratories

Issued by Sandia National Laboratories, operated for the United States Department of Energy by Sandia Corporation.

Printed in the United States of America. This report has been reproduced directly from the best available copy.

Available to DOE and DOE contractors from
U.S. Department of Energy
Office of Scientific and Technical Information
P.O. Box 62
Oak Ridge, TN 37831

Telephone:	(865) 576-8401
Facsimile:	(865) 576-5728
E-Mail:	reports@adonis.osti.gov
Online ordering:	http://www.osti.gov/bridge

Available to the public from
U.S. Department of Commerce
National Technical Information Service
5285 Port Royal Rd.
Springfield, VA 22161

Telephone:	(800) 553-6847
Facsimile:	(703) 605-6900
E-Mail:	orders@ntis.fedworld.gov
Online order:	http://www.ntis.gov/help/ordermethods.asp?loc=7-4-0#online

SAND2014-0779
Unlimited Release
Printed January 2014

Evaluation of Select Heat and Pressure Measurement Gauges for Potential Use in the NRC/OECD High Energy Arc Fault (HEAF) Test Program

Carlos Lopez
Structural and Thermal Analysis Department

William B. Wente
Energetic Component Engineering Department

Victor G. Figueroa
Structural and Thermal Analysis Department

Sandia National Laboratories
P.O. Box 5800
Albuquerque, New Mexico 87185-MS0718

Abstract

In an effort to improve the current state of the art in fire probabilistic risk assessment methodology, the U.S. Nuclear Regulatory Commission, Office of Regulatory Research, contracted Sandia National Laboratories (SNL) to conduct a series of scoping tests to identify thermal and mechanical probes that could be used to characterize the zone of influence (ZOI) during high energy arc fault (HEAF) testing. For the thermal evaluation, passive and active probes were exposed to HEAF-like heat fluxes for a period of 2 seconds at the SNL's National Solar Thermal Test Facility to determine their ability to survive and measure such an extreme environment. Thermal probes tested included temperature lacquers (passive), NANMAC thermocouples, directional flame thermometers, modified plate thermometers, infrared temperature sensors, and a Gardon heat flux gauge. Similarly, passive and active pressure probes were evaluated by exposing them to pressures resulting from various high-explosive detonations at the Sandia Terminal Ballistic Facility. Pressure probes included bikini pressure gauges (passive) and pressure transducers. Results from these tests provided good insight to determine which probes should be considered for use during future HEAF testing.

Acknowledgments

The authors gratefully acknowledge and thank Cheryl Ghanbari, Sylvia Gomez, H. Lee Stauffacher, Robert Jones, all from Sandia, and Randall Foster of Technical Management SolutionS (TMSS), Inc., for their outstanding support and assistance throughout the test series. The authors would also like to thank Douglas J. Ammerman (Sandia) for the technical review of this document and Walter Gill (Sandia) for his technical advice and assistance with the thermal instrumentation, interpretation of the data, and for the technical review of this document. The authors specially acknowledge and thank Gabriel J. Taylor and Mark Henry Salley, our sponsors in the Fire Research Branch at the U.S. Nuclear Regulatory Commission (NRC), for their guidance and support for fire PRA programs. Funding for this work was provided through NRC Job Code N6981.

Contents

Figures

Tables

1 Introduction

Electrical power and distribution components such as switchgears, load centers, and bus bars are subject to potential failure based on large electrical shorting discharges characterized as high energy arc fault (HEAF) events. These faults have the potential to cause extensive damage to the failed electrical component and distribution system along with adjacent equipment and electrical cables. Operating experience has demonstrated that the high temperatures generated during HEAF events have ignited combustible components inside and outside the cabinet and have led to total cabinet destruction with pressures large enough to physically deform cabinets, breach cabinet doors, and even project cabinet panels several feet away. The significant energy released during a HEAF event can also act as an ignition source to other nearby components.

HEAFs continue to occur in nuclear power plants (NPP) throughout the world. The current state of the art method for quantifying the risk of these HEAFs is documented in Appendix M of NUREG/CR-6850, "EPRI/NRC-RES Fire PRA Methodology for Nuclear Power Facilities." This method defines a HEAF zone of influence (ZOI) as the physical region where equipment will be damaged, or ignition will occur to a fire PRA target component. This ZOI method is based on the information available from a small data set of 12 HEAF events in the US commercial nuclear industry between 1979 and 2001 including, most notably, a 2001 event at the San Onofre Nuclear Generating Station.

Appendix M in NUREG/CR-6850 delineates the HEAF event into two phases: an energetic phase and an ensuing fire phase. One of the key components in addressing a HEAF event is characterizing the damage during the energetic phase of the event. The enclosure in which a HEAF event occurs may be breached by the explosive release of energy. This factor greatly influences the immediate heat flux to which nearby objects are exposed. The ensuing fire phase is also of interest, as it can be the cause for fire spread and failure of additional components and equipment that was not damaged by the initial HEAF event. One of the major limitations to Appendix M is that it presents a "one size fits all" model. That is, provided a component meets the criteria for a HEAF event, there is no further distinction made based on the characteristics of the specific initiating component (e.g., voltage or current level, device type, etc.) nor those of the component's enclosure (e.g., robustness of the surrounding enclosure). Thus, regardless of the electrical enclosure purpose (load center, motor control center, medium voltage switchgear, etc.) the ZOI does not change in the current quantification method.

In an effort to improve the current state of the art in fire probabilistic risk assessment (PRA) methodology, the U.S. Nuclear Regulatory Commission (NRC), Office of Regulatory Research (RES), has contracted with Sandia National Laboratories (SNL) to participate in a confirmatory testing program that will be evaluating different types of equipment and voltage levels to better characterize the ZOI for HEAF events. This program is being conducted in collaboration internationally with the Organization for Economic Co-operation and Development (OECD). To capture valuable data from this testing, it is first necessary to identify and evaluate the instrumentation that will be used to measure heat fluxes and pressures generated by various HEAF events. Provided that HEAFs are generally of short duration, probes used to make the temperature and pressure measurements need to be fast responding but, at the same time, robust to withstand the effects of large electrical discharges (*i.e.*, large electrical and electromagnetic fields, very fast thermal shock, pressure bursts, very hot shrapnel, vibrations, and heat from secondary fires). The requirements for a probe to make these measurements are:

1) obtain information about the arc without being damaged by the arc and ejected debris,
2) function properly during the tests,
3) minimize the effects of electrical noise in the acquired data, and
4) ensure proper function and protection of the data acquisition system.

This document describes a series of scoping tests that were performed at SNL to evaluate various instruments for potential application during future HEAF testing. The primary objective of this instrumentation test series is to evaluate different heat flux and pressure measuring probes and techniques that may be used to better understand the effects of HEAF events on the enclosure in which it occurs, on adjacent fire PRA target components, and the effects of a possible ensuing fire. Candidate probes were identified and then exposed to simulated short duration high heat flux and high-pressure conditions. The high heat fluxes were obtained at the SNL solar tower and the high-pressure conditions were obtained using explosives. Testing the instruments with these simulated exposures was done to *explore* if these are adequate probes for use in future HEAF testing for the collection of experimental data. The remainder of this report documents the instrument and experimental design used to evaluate the effectiveness of various passive and active pressure and thermal instruments.

2 General Description of the Instrumentation

In the preliminary screen for candidate probes, consideration was given to the effects of high energy sources and short circuits, causing noise in measurements, probe malfunction, and/or damage to the data acquisition (DAQ) system . Therefore, passive gauges that do not consist of electronics or need electrical power may provide useful information for any instance where data from the active gauges are rendered unusable. In this series of experiments, both passive and active thermal probes were put forth. The probes that were investigated are described in Table 1. Figure 1 through Figure 9 provide examples of the probes described in this table.

A series of experiments were conducted to identify reliable methods of obtaining the data necessary to confirm and improve the state of the art methods for modeling HEAF events in fire PRAs. Instrument tests were designed to expose the different types of probes to thermal and mechanical environments similar to those generally observed in HEAFs. As such, heat and temperature probes were exposed to very large changes in heat flux for a very short period of time using the SNL solar tower. In addition, pressure and thermal probes were exposed to explosive mechanical loads at the SNL Terminal Ballistic Facility (TBF).

By testing different types of probes under controlled conditions, it was possible to compare probe performance and identify which probes are more likely to capture and record the data needed to characterize ZOI during actual HEAF tests in the future. Note that this was a scoping effort aimed at identifying probes that could survive and respond fast enough to capture the abnormal thermal and mechanical conditions observed in HEAF testing. Since this was a discovery effort, uncertainties in the measurements were not thoroughly investigated. Instead, calibrated probes were used to make general observations about the quality of the data collected by the non-calibrated probes that were evaluated. Probes that, based on the results of this effort, are identified for use in actual HEAF testing will be calibrated so that uncertainties can be better quantified in future efforts.

Table 1. List of passive and active gauges evaluated

Gauge Type	Probe or Gauge	Description
Passive	Bikini Pressure Gauge (Figure 1)	Two plates with a series of holes of different sizes sandwich a thin sheet of aluminum foil. Each aluminum foil disc will rupture at a different blast pressure exposure. This probe can be used to obtain an estimate of peak pressure observed.
	Temperature Lacquers (Figure 2)	Special lacquers that respond to different temperatures (i.e., change state and/or finish) and can be used to estimate peak temperatures observed at different locations.
	Cable Coupons (Figure 3)	Short segments of thermoplastic and thermoset cables were added to the instrumentation panels to provide anecdotal cable response evidence.
Active	NANMAC Corporation E6 Series TCs (Figure 4)	These are fast responding thermocouples (with self-renewing junction) that can be mounted on a block of steel. This assembly can be used as heat flux gauge by fitting a heat transfer model that represents a semi-infinite solid in terms of heat transfer.
	Plate Thermometers (Figure 5)	These gauges are typically used to obtain estimates of temperature and heat flux from fires.
	Directional Flame Thermometers (Figure 6)	These gauges are typically used to obtain estimates of temperature and heat flux from fires. They are similar to plate thermometers.
	Infrared Temperature Sensor (Figure 7)	Active gauge used to measure temperature through infrared emissions “without contacting” the surface from which temperature is being measured.
	Gardon Gauge (Figure 8)	A water-cooled circular foil heat flux sensor designed to measure high intensity hemispherical radiative heat flux.
	Pressure Transducers (Figure 9)	These active gauges generate an electrical signal as a function of the pressure imposed. Fast-response gauges will be used for the tests.

Figure 1. Bikini pressure gauge

Figure 2. OMEGALAQ ® liquid temperature indicators in bottles (left) and as applied on thin plate (right)

Figure 3. 9 cm (3.5 in) long cable segments (one thermoset and one thermoplastic)

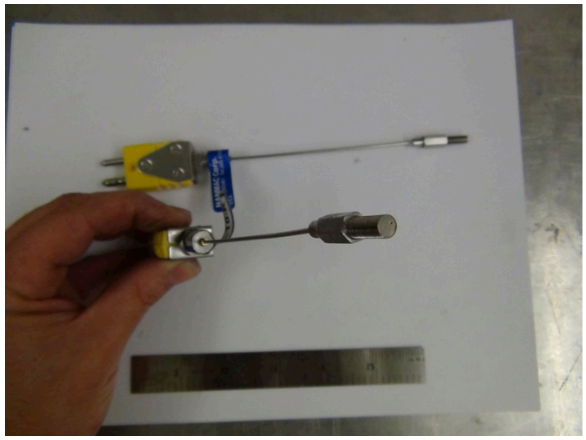

Figure 4. NANMAC thermocouple

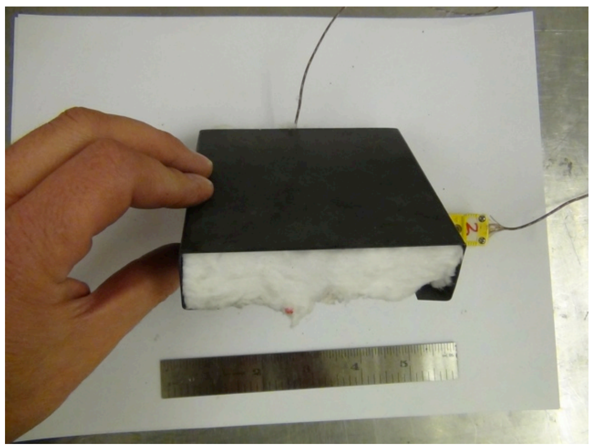

Figure 5. Plate thermometer

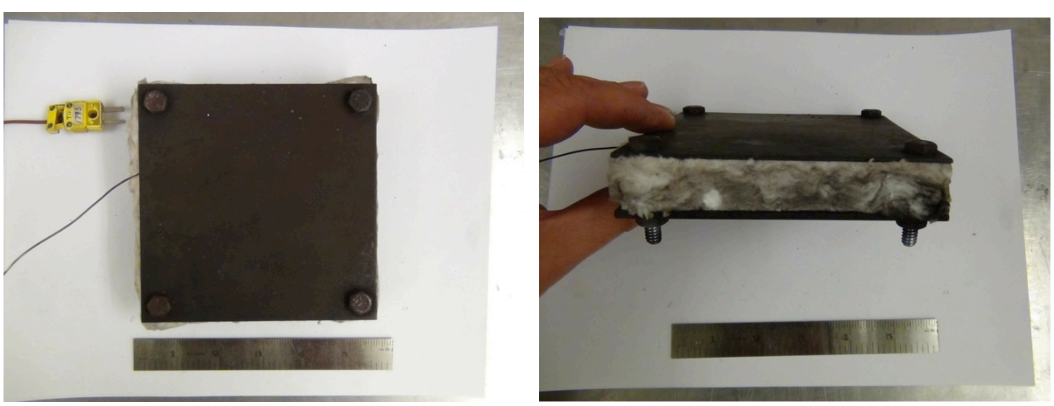

Figure 6. Directional flame thermometer

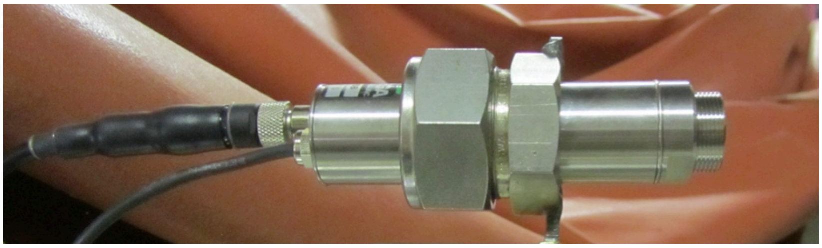

Figure 7. Infrared temperature sensor

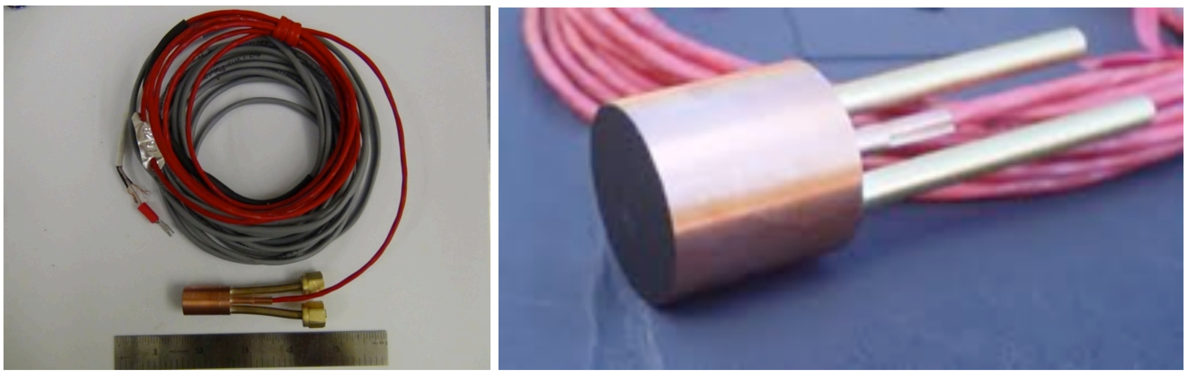

Figure 8. Gardon gauge

Figure 9. Pressure transducer: Pencil gauge being installed on a tripod before testing (left) and as installed on tripod (right)

3 High Heat Flux Tests: Description and Summary of Results

HEAF events are known to produce extremely high heat fluxes over very short time frames of milliseconds to a few seconds, depending on the characteristics of the system and electrical fault. For this test series, heat fluxes ranging from 0.5 to over 2 MW/m^2 were selected based on IEEE 1584 heat release calculations using voltages ranging from 480 V to 7.2 kV and short circuit currents ranging from 20 to 40 kA. A nominal test duration of 2 seconds was selected based on the understanding that the more damaging HEAFs are those that last over one second and also considering the duration of the HEAFs that a power testing facility can support at the desired voltages and amperages during future HEAF testing. While two seconds was the heat exposure duration chosen for these scoping tests, the probes that were evaluated are capable of measuring the heat fluxes from shorter and longer duration HEAFs and should be suitable for use in the HEAF tests that are planned for the future. Step change heat flux profiles maintained over 2 seconds were used to simulate HEAF environments.

To achieve these profiles, the Solar Tower and the heliostat field at the National Solar Thermal Test Facility (NSTTF) at SNL were used. The Solar Tower is a 61 m (200 ft) high concrete structure with three test locations. The heliostat field has 218 individual heliostats that can provide flux levels exceeding 3 MW/m^2 and total power in excess of 6 MW. Pictures taken during and between the tests discussed here are shown in Figure 10.

For this test series, the high-speed shutter in the test bay that is 43 m (140 ft) above the ground was used. Using the heliostats alone, the time required to reach 100% flux is about 3.5 seconds. The shutter allows for the sudden high intensity heat flux exposure to samples requiring a step change heating profile. A calibration target, located next to the shutter, is used to evaluate the flux profile and measure the heat flux level that the target will be exposed to before and after each sample exposure. The shutter aperture is about 127 cm wide by 91 cm tall (50 in by 36 inches). The shutter has two doors that open horizontally with an opening time of 0.15 seconds. For these tests, it was desired to expose the samples for a minimum of 2 seconds. The actual exposure time to each sample was 2.4 seconds. The extra 0.4 seconds were enough to account for the 0.3 seconds associated with opening and closing of the shutter and guarantee a two-second full sample exposure.

(a) Solar energy concentrated on the test bay used for these tests

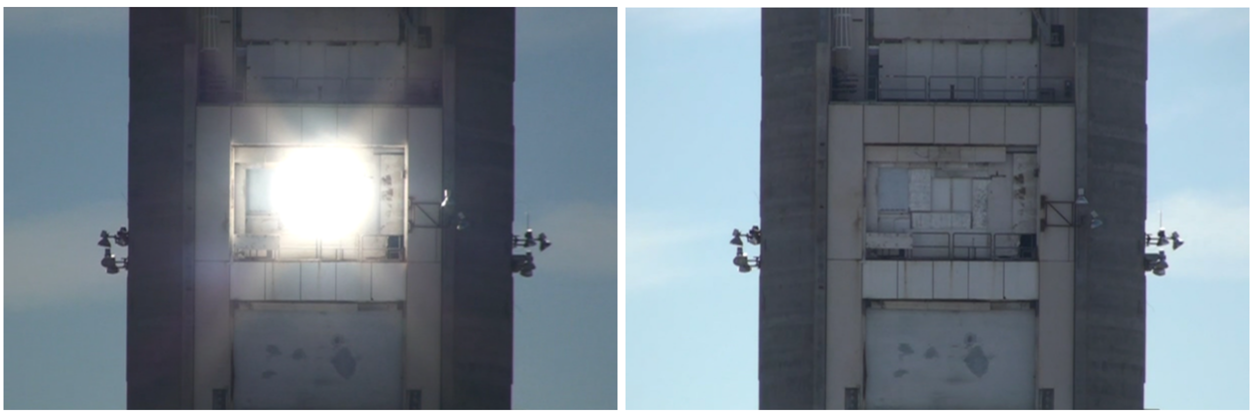

(b) Close-up of the test bay 43m (140 ft) above the ground during (left) and after test (right)

(c) Shutter in the open position (left) and array of heliostats used for these tests (right)

Figure 10. High heat flux testing at SNL's Solar Tower test facility

3.1 Instrumentation for high heat flux test

A metal frame shown in Figure 11 was designed to hold a combination of passive and active gauges for the high heat tests at the SNL Solar Tower[1]. This frame allowed for the easy interchange and modification of probes between tests. As shown in the figure, the frame has four locations where combinations of plate thermometers, directional flame thermometers (DFTs), flat plates for infrared temperature measurements, or metal plates with temperature lacquer were assembled. In addition, the frame has permanent locations for a NANMAC thermocouple (center hole of the 6.4 cm (2.5 in) stainless steel disk that is in the middle vertical bar) and a Gardon gauge (lower hole in the middle vertical bar). The NANMAC and the Gardon gauge can be seen more clearly in Figure 12. As shown in the figure, the centers of these gauges are equidistant from the horizontal centerline of the frame. The frame with installed instrumentation is referred to in this document as "instrumentation cluster." The overall dimensions of the instrumentation cluster are 28 cm by 43 cm (11 in by17 in). Fully assembled instrumentation clusters used for testing are shown later.

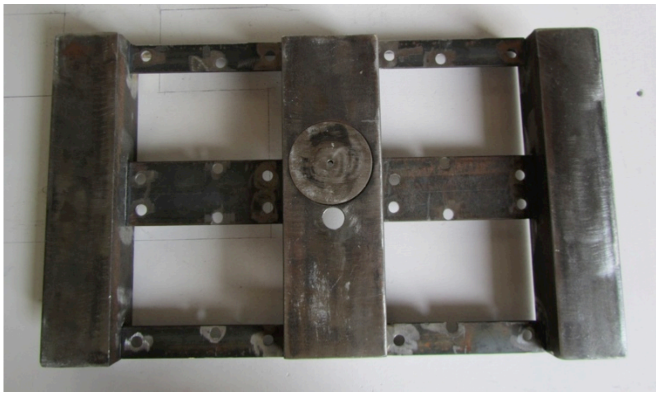

Figure 11. Metal frame used to hold heat probes during testing

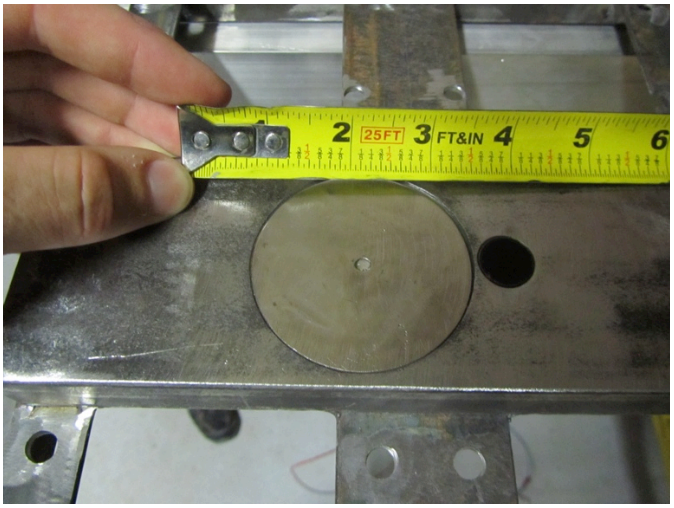

Figure 12. Close-up on the installed NANMAC (left) and Gardon gauge (right)

---

[1] A concentrating solar test facility at Sandia National Laboratories described in more detail later in this report.

An instrumentation cluster typical of the ones used during this test series is shown in Figure 13. In this picture, a technician is installing a DFT in one of the quadrants of the metal frame before exposing the completed instrumentation cluster to a high heat flux test. Mounted on that particular cluster are two plate thermometers of different plate thickness, two DFT with different thermocouple mounting techniques, one NANMAC, and one Gardon gauge. Therefore, one instrumentation cluster accommodated six different measuring devices.

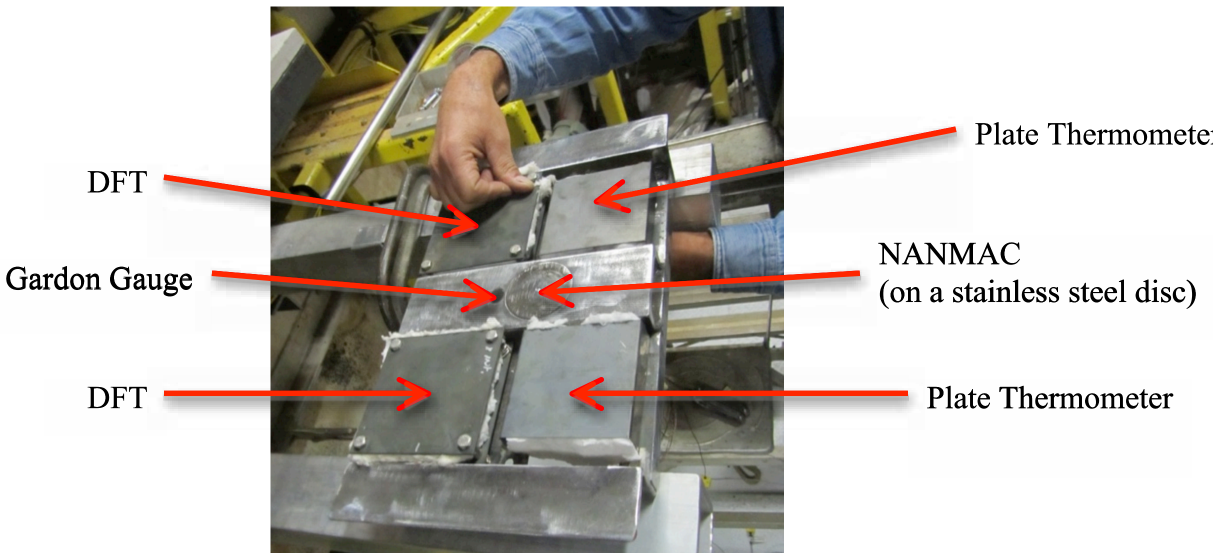

Figure 13. Instrumentation cluster typical of this test series

Instrumentation clusters similar to the one shown in Figure 13 were assembled for the tests at the SNL Solar Tower. Plate thermometers made out of Inconel 600 were designed to measure a large temperature variation during the two-second heat exposure.

3.2 High heat flux test setup and test matrix

The setup at the SNL Solar Tower consisted of one instrumentation cluster per test. A total of nine tests were conducted to cover a range of heat exposure and probes being tested. Tests were performed at four nominal heat flux levels: 0.5, 1.0, 1.5, and 2.0 MW/m^2. Two tests were conducted at each heat exposure level (for a total of eight) to allow for the evaluation of all the thermal probes described earlier in this document. An additional test was performed at the 2 MW/m^2 level to expose the Bikini gauge to the high heat and determine if it is possible to discern between mechanical or thermal damage to the aluminum foil that is a part of the probe. The test matrix with the probes used and their position for each test is shown in Figure 14. Note that in this figure, the NANMAC and the Gardon probes are not identified, but are present in Tests 1 through 8. In addition, in this figure “18mil,” “25mil,” and “65mil” refer to the thickness (in 1/1000 inch) of the Inconel ™ plate used to either: 1) mount an intrinsic[2] or a sheathed thermocouple to make a plate thermometer (PT), 2) read its temperature with an infrared sensor

[2] An intrinsic thermocouple is made by electrically fusing the two thermocouple wires separately to a metal surface, effectively making the mounting surface the sensing junction of the thermocouple.

(“IR”), or 3) apply the OMEGALAQ® liquid temperature indicator (LAQ). DFTr and DFTi refer to regular and intrinsic directional flame thermometer, respectively. The DFTr is instrumented with a sheathed thermocouple and the DFTi has an intrinsic thermocouple. Besides these probes, plates of different thickness on which the OMEGALAQ® liquid temperature indicator was applied are referred to as 18, 25, and 65 mil “LAQ.” Finally, there were some tests in which thermoset and thermoplastic multi-conductor control cable segments (both 7-conductor, 12 AWG) were exposed to the high heat and those are identified in this figure as “Cables.”

Test 1 - 0.5 MW/m²:

18mil PT	25mil PT
DFTr	DFTi

Test 2 - 0.5 MW/m²:

18mil PT Sheathed	Cables
18mil IR	18mil LAQ

Test 3 - 1 MW/m²:

18mil PT	25mil PT
18mil IR	DFTi

Test 4 - 1 MW/m²:

18mil LAQ	Cables
25mil IR	25mil LAQ

Test 5 - 1.5 MW/m²:

25mil PT	DFTi
65mil IR	25mil PT Sheathed

Test 6 - 1.5 MW/m²:

65mil LAQ	Cables
25mil IR	25mil LAQ

Test 7 - 2 MW/m²:

DFTr	Cables
65mil IR	DFTi

Test 8 - 2 MW/m²:

DFTr	65mil LAQ
65mil IR	DFTi

Test 9 – 2 MW/m² - Bikini gauge only:
The portion of the gauge that was exposed to the heat had both pristine and broken aluminum foil.

Figure 14. Solar Tower test matrix (heat flux levels are nominal)

3.3 High heat flux test results and discussion

The test log of heat flux exposures for the tests matrix in Figure 14 is shown in Table 2. This table shows the flux levels that were measured just before and just after each two-second exposure test by a reference probe (a Kendall Mk IX radiometer) that is mounted on the exterior of the SNL Solar Tower within the testing focal point for the heliostat array. These secondary pre- and post-test heat flux measurements were used as indicators of the heat exposure levels in each test. Actual test flux exposures were measured with gauges mounted on the instrumentation cluster.

Table 2. Solar Tower pre- and post-test calibration log

Date	Time	Exposure #	Number of Heliostats	Heat Flux Level
10/2/2012	12:30	Exposure #1	24	Pre-test cal: 578 kW/m^2 Post-test cal: 578 kW/m^2
	13:24	Exposure #2a*	24	Pre-test cal: 591 kW/m^2 Post-test cal: 580 kW/m^2
	13:50	Exposure #2b	24	Pre-test cal: 555 kW/m^2 Post-test cal: 553 kW/m^2
	14:31	Exposure #3	52	Pre-test cal: 1,132 kW/m^2 Post-test cal: 1,093 kW/m^2
	14:57	Exposure #4	60	Pre-test cal: 1,152 kW/m^2 Post-test cal: 1,109 kW/m^2
10/4/2012	12:16	Exposure #5	72	Pre-test cal: 1,754 kW/m^2 Post-test cal: 1,699 kW/m^2
	12:42	Exposure #6	72	Pre-test cal: 1,655 kW/m^2 Post-test cal: 1,743 kW/m^2
	14:00	Exposure #7	120	Pre-test cal: 2,173 kW/m^2 Post-test cal: 2,250 kW/m^2
	14:32	Exposure #8	136	Pre-test cal: 2,217 kW/m^2 Post-test cal: 2,129 kW/m^2
	14:55	Exposure # 9: Bikini gauge only	136	Pre-test cal: 2,052 kW/m^2 Post-test cal: 2,030 kW/m^2

* No thermocouple data was collected during Test 2a. The data collected during Test 2b is presented in this document as Test 2 data.

Figure 15 through Figure 18 show the temperatures measured during all tests. Note that the temperature readings from the probes that were instrumented with sheathed thermocouples (i.e., PTs identified as “Sheathed” in Figure 14 and all DFTr) continued to rise even after the solar heating was removed. This indicates that the measurements on those probes lagged the actual response of the plate. Provided that the goal is to use probes that can measure the heat from HEAF events that last for about two seconds, the response of those probes would be too slow and are, therefore, deemed as not adequate for use in that application. Since the heat flux cannot be estimated with any confidence from those probes, only their temperature (and not heat flux) responses are presented in this document. In the case of the IR, the probe had a limited sampling rate of 1 Hz (or one sample per second). That limitation rendered the data from that probe unusable for inverse heat transfer calculations because only two or three data points are available during the heat exposure time. Small measurement errors in that small set of data could lead to very large errors in heat flux estimates. For this reason, only their temperature readings and not any inferred heat flux are presented in this document.

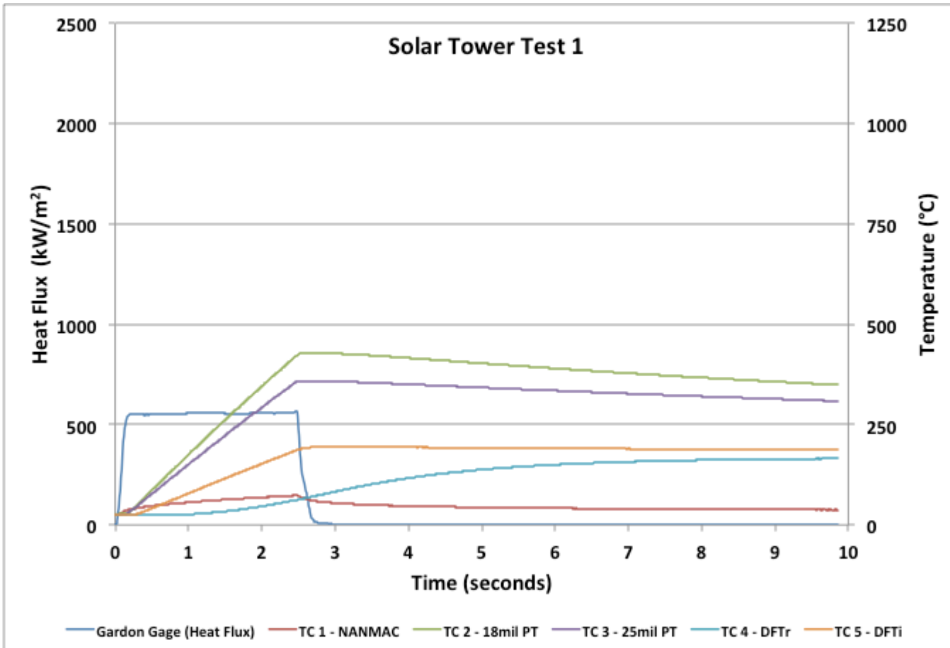

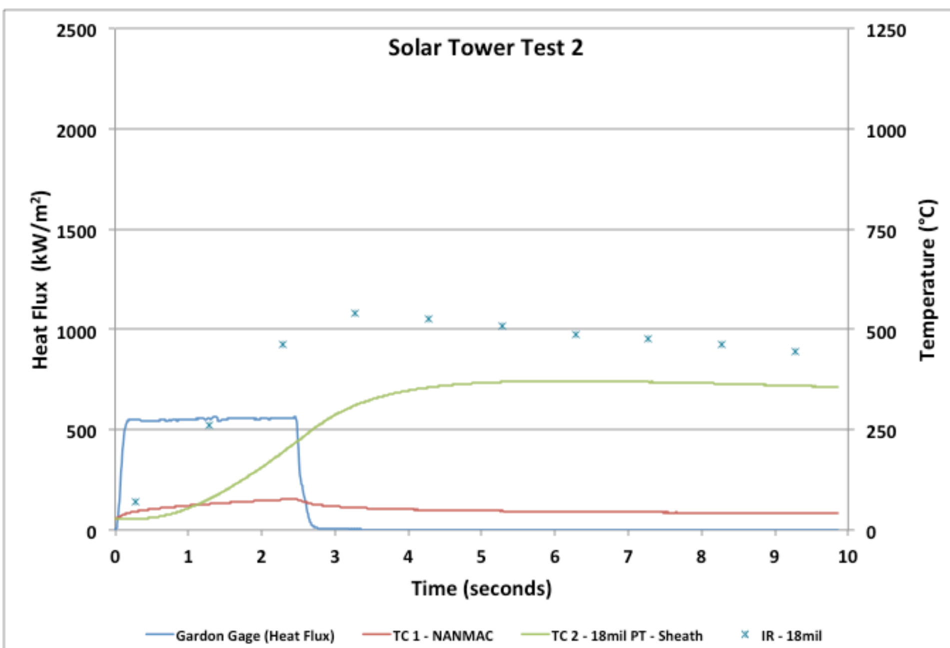

Figure 15. Heat and temperature data from Tests 1 and 2 (0.5 MW/m^2 nominal exposure)

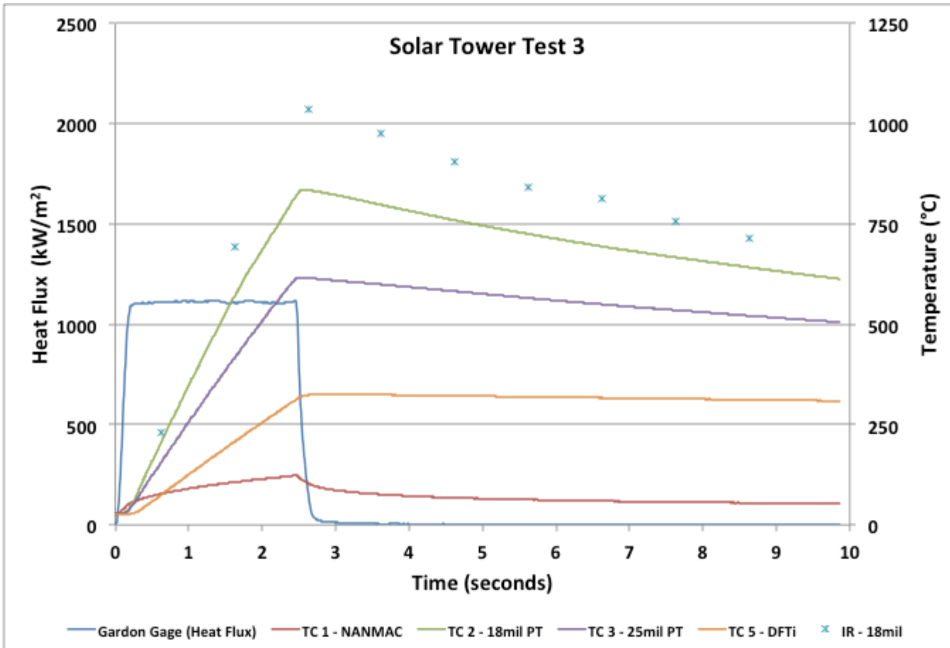

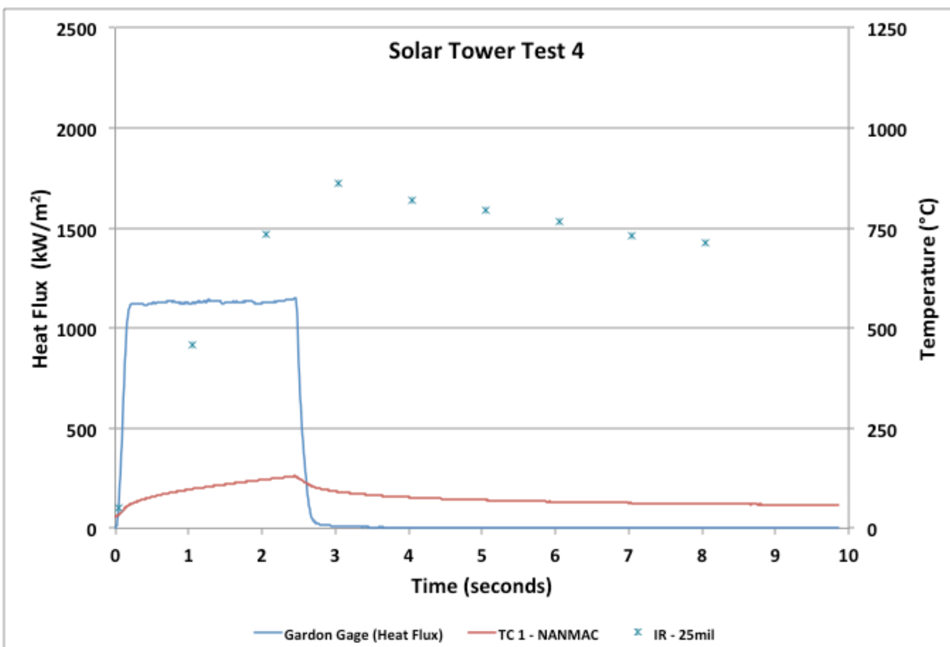

Figure 16. Heat and temperature data from Tests 3 and 4 (1 MW/m^2 nominal exposure)

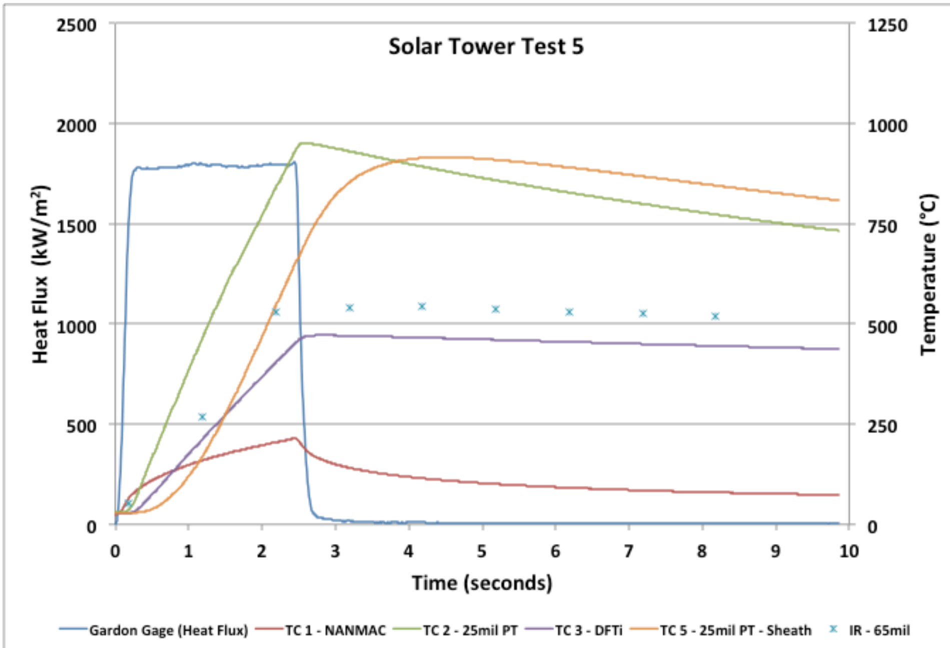

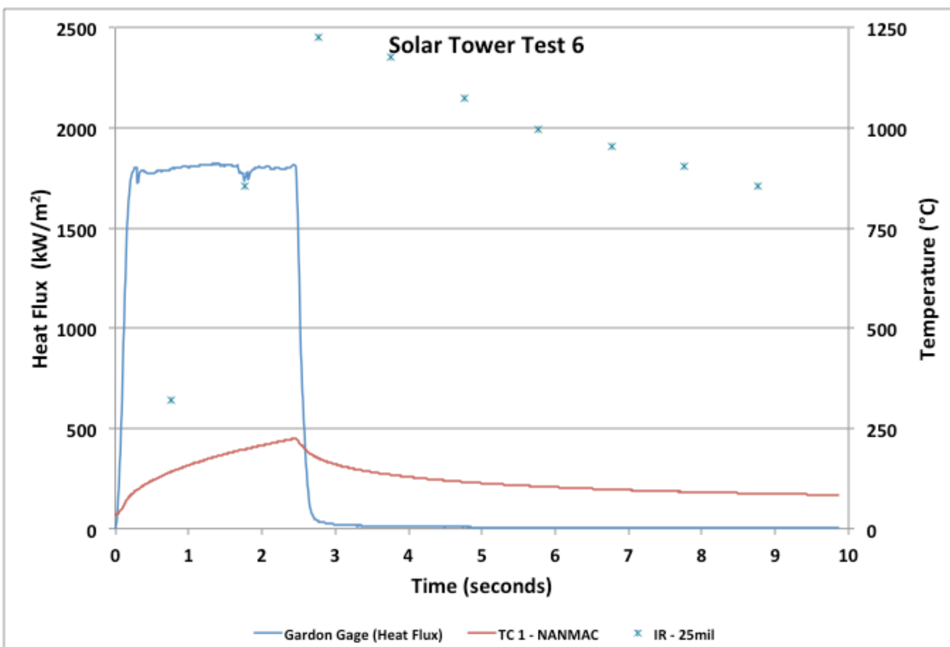

Figure 17. Heat and temperature data from Tests 5 and 6 (1.5 MW/m^2 nominal exposure)

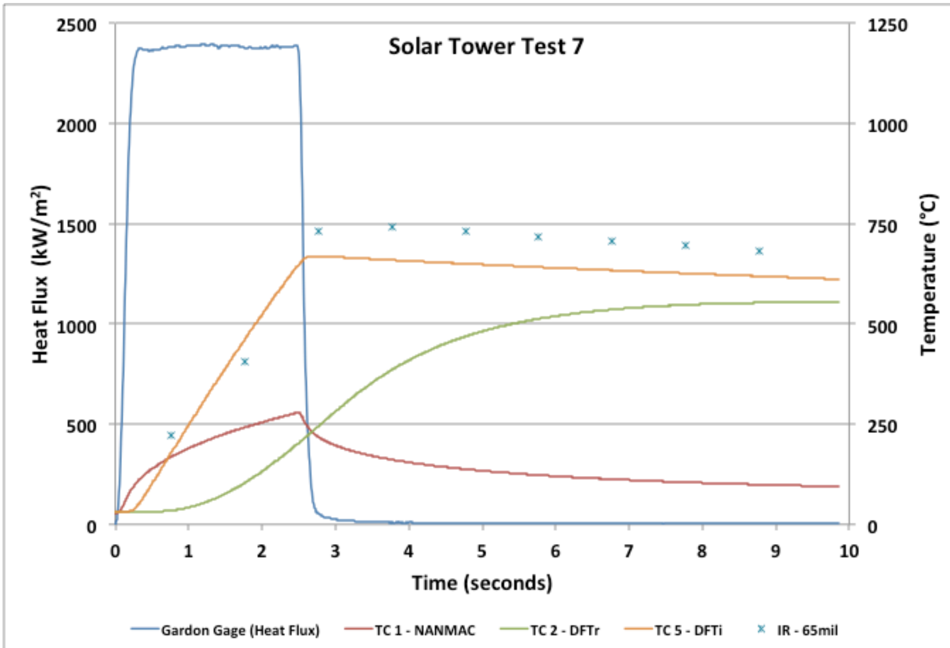

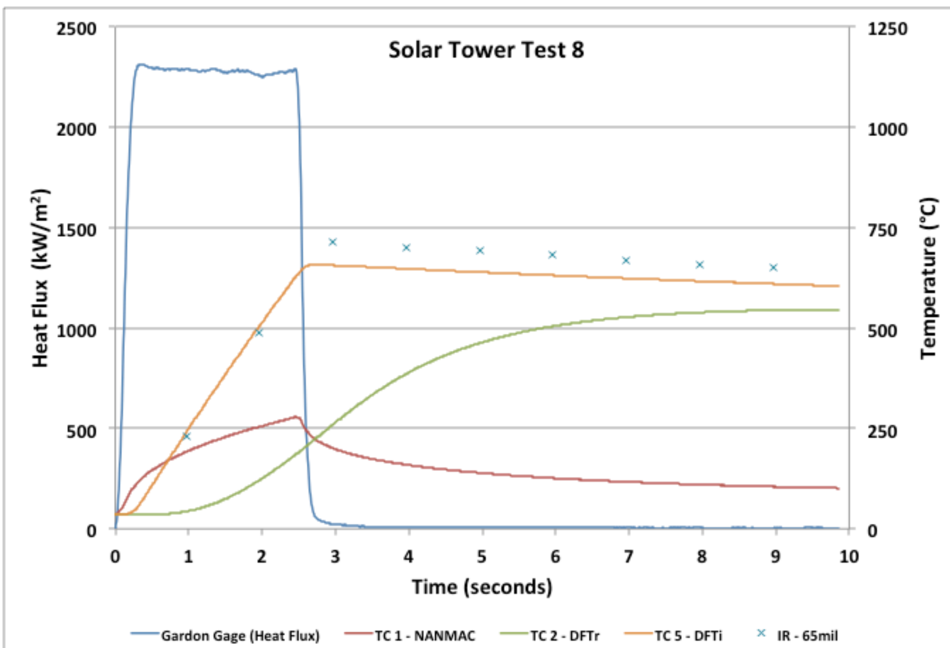

Figure 18. Heat and temperature data from Tests 7 and 8 (2 MW/m^2 nominal exposure)

As previously stated, five different types of probes were used during this test series to obtain heat flux. The Gardon gauge and NANMAC thermocouple were the only gauges used in all tests. The Gardon gauge was taken as the reference gauge because it is calibrated to a known blackbody heat source, responds fast to a heat exposure, measures heat flux based on the temperature rise of an exposed flat surface as is the case of the probes that are being evaluated and calibrated in this effort, and because it was mounted on the same fixture with the rest of the instrumentation cluster. The Gardon gauge directly measures the incident heat flux with a simple voltage-to-heat-flux relation. However, this gauge requires cooling and some protection in extreme environments, which makes them less attractive for use in HEAF testing.

Backside (unexposed side) temperature readings from plate thermometers and DFTs were used in inverse heat conduction [1] calculations to estimate the temperature of the front (i.e., exposed or sensing) surface and the absorbed heat flux of the probe. The inverse heat conduction calculations were completed using the IHCP1D computer program [2]. Temperature-dependent properties for Inconel 600 and for the Cerablanket® insulation used in the fabrication of the plate thermometers and DFTs were considered in the inverse heat conduction calculations. The thermophysical properties used are presented in Appendix A. To estimate the heat flux absorbed by the NANMAC assembly, the temperature solution for a semi-infinite solid exposed to a constant surface heat flux [3] was fitted to the temperature response of the probe using a least squares, error minimization, iterative technique. Through this technique, one finds the constant heat flux exposure that leads to the temperature history measured by the NANMAC assembly.

With all these probes, the emissivity of the sensing surface is required to transform the calculated absorbed heat flux to an incident heat flux. It has been found that the resulting incident heat flux is sensitive to the total hemispherical emissivity used in the transformation, and since this integrated emissivity is a function of the condition and temperature of the surface, it is difficult to obtain reliable values. In most cases, reliable methods of measuring the temperature-dependent hemispherical emissivity are expensive. Simplified emissivity measurements at ambient conditions are more commonly used but could lead to relatively large errors (on the order of tens of percent) when used to estimate incident heat flux on surfaces that are at much higher temperatures than ambient. Measuring temperature-dependent emissivities can be very expensive and was not a part of this scoping study.

For these reasons, an alternate approach that does not depend on direct emissivity input values was used to estimate the incident heat flux as measured by the NANMAC assembly, the DFTs, and the plate thermometers. Absorbed heat fluxes (q''_{absorbed}) obtained for each of the above-mentioned measurement techniques were translated to incident heat flux using the incident heat flux (q''_{incident}) as measured by the Gardon gage in Test 1. That is, the effective absorptivity ($\alpha_{\text{effective}}$) of each sensing face was obtained by calculating the ratio of the absorbed heat flux to the measured incident heat flux as measured by the Gardon gauge (see Equation 1).

$$\frac{q''_{\text{absorbed}}}{q''_{\text{incident}}} = \alpha_{\text{effective}} \qquad \text{(Eq. 1)}$$

where;

q''_{absorbed} = heat flux absorbed by the gauge being calibrated
q''_{incident} = incident heat flux as measured by the Gardon gauge
$\alpha_{\text{effective}}$ = estimated effective absorptivity of the gauge being calibrated

The underlying assumption made here is that convection effects were minimal during these tests. Since both the absorbed and incident heat fluxes varied slightly with time during each test, average values calculated from the data acquired between 0.5 and 1.0 seconds into the test (while the shutter was fully opened) were used to estimate the effective absorptivity for the NANMAC, the plate thermometer, and the DFT used in the tests. These absorptivity values were then used to estimate the incident heat flux (q''_{incident}) as "measured" by each probe in subsequent tests. This is represented in Equation 2.

$$\frac{(q''_{\text{absorbed}})_{test\_i}}{(\alpha_{effective})_{test\_1}} = (q''_{\text{incident}})_{test\_i} \qquad \text{(Eq. 2)}$$

where;

$(q''_{\text{absorbed}})_{test\_i}$= heat flux absorbed by a gauge at particular test
$(\alpha_{effective})_{test\_1}$= estimated effective absorptivity of the gauge based on Test 1
$(q''_{\text{incident}})_{test\_i}$ = estimated incident heat flux

Since the above calibration technique is acceptable as long as the same NANMAC, plate thermometer, and DFT are used, the effective absorptivity of the NANMAC sensing surface had to be recalculated starting in Test 5 because a different NANMAC thermocouple was used starting with that test. All other measurement techniques (PTs and DFTs) continued to use the same effective absorptivity value calculated in Test 1, as the probes used were the same.

Figure 19 through Figure 22 show the incident heat flux estimates for all tests. Note that, as explained earlier in this document, only heat flux estimates from the probes that had a timely response to the heating exposure are presented in these plots. In addition, the constant heat flux estimated using the NANMAC assembly is shown as a horizontal line in these plots. These results show very good agreement between all the probes used in Test 1, as this was the test used to calibrate the other probes. However, as those calibration factors were used for other tests, deviations from the Gardon gauge readings were observed. The NANMAC was the probe that remained closest to the Gardon gauge readings. The plate thermometers and the DFT seemed to be more affected by other heat transfer effects such as radiation and convection heat loss to the environment, especially as the magnitude of the heat exposure was increased. Both of these gauges are of much less thermal mass than the NANMAC configuration and, when they were heated, their temperature increased much more than the NANMAC configuration did (see Figure 15 through Figure 18). The plate thermometers and the DFT were designed to sense fast heating and respond in this manner. However, the larger temperature differences with respect to the environment lead to higher heat losses. For example, the highest temperature measured by the 25-mil plate thermometer in Test 5, a 1500 kW/m^2 test, was about 950ºC, which implies that one can estimate peak heat loss by convection of about 5-10 kW/m^2 (assuming a natural convection heat transfer coefficient of 5-10 W/m^2-K) and a peak heat loss by radiation of about 115 kW/m^2 (assuming a high surface emissivity of 0.9). In this example, the error introduced by not accounting for convection and radiation heat losses is on the order of 8% [or (10 kW/m^2 +115 kW/m^2)/(1500 kW/m^2) x 100] for the conditions of that test.

Passive temperature indicators were also used to estimate peak temperature. Lacquers with different temperature setpoints were applied wet on the back surface of plates of different thickness and allowed to dry before testing. The manufacturer specifies that once the lacquers dry they have a dull-opaque appearance and when their set temperature is reached they melt and look glossy-transparent. An advantage of using these lacquers is that they can provide a peak temperature reading without the need for instrumentation. Some of the disadvantages include: 1) transient data is not captured, 2) it can be difficult to determine which lacquers have reached their set temperature, and 3) the resolution of the reading is only as good as the difference between the highest lacquer set temperature reached and the next (higher set temperature) lacquer that did not reached its set temperature. Table 3 shows the peak temperature readings that were estimated following manufacturer's specifications on how to read the lacquers. The manufacturer specifies an accuracy of ±1% and a response time on the order of milliseconds. However, such accuracy was not observed during these tests. That is, the temperature readings shown in Table 3 are not in good agreement with other readings made on plates of the same thickness exposed to the same nominal heat flux. Surprisingly, only one reading seemed to agree with the temperature read by an active gauge despite the accuracy claimed by the manufacturer (+/- 1%). A column with peak temperatures as read by active gauges was added to Table 3 to illustrate the differences in the readings. Once again, the readings by the active gauges shown in this table were obtained from plates of the same thickness and exposed to the same nominal (not necessarily exact) heat flux.

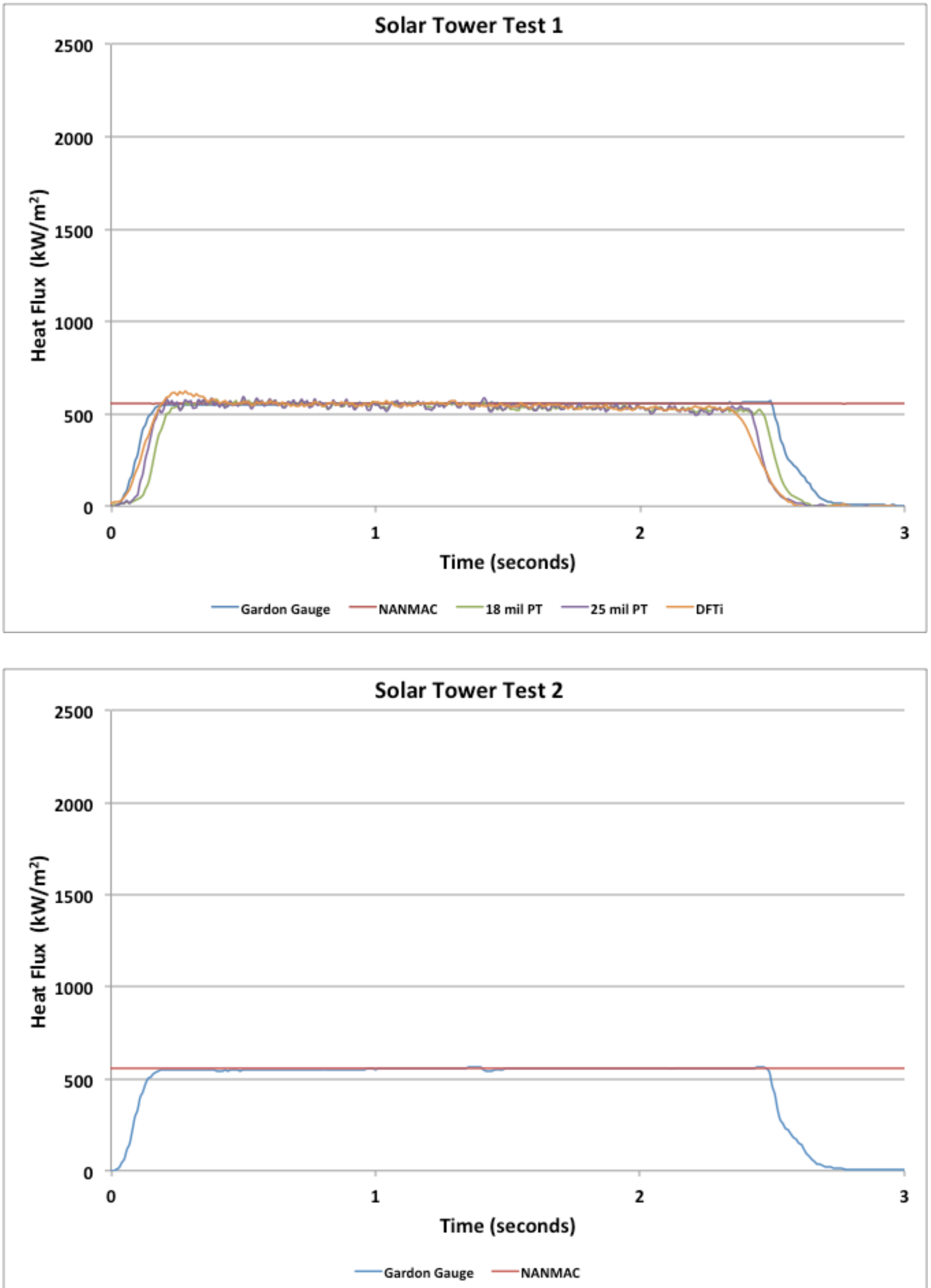

Figure 19. Heat flux estimates for Tests 1 and 2 (0.5 MW/m^2 nominal exposure)

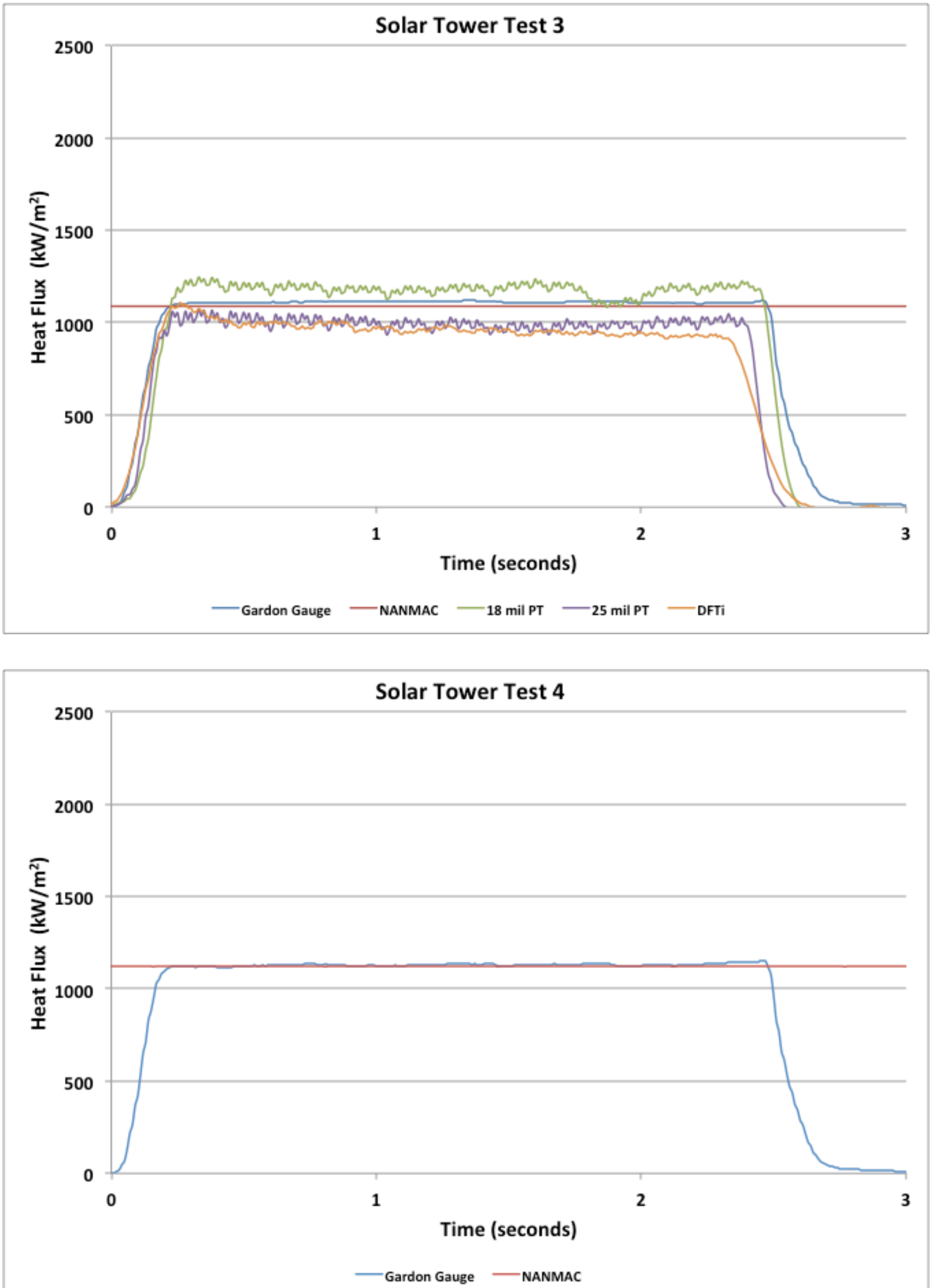

Figure 20. Heat flux estimates for Tests 3 and 4 (1 MW/m^2 nominal exposure)

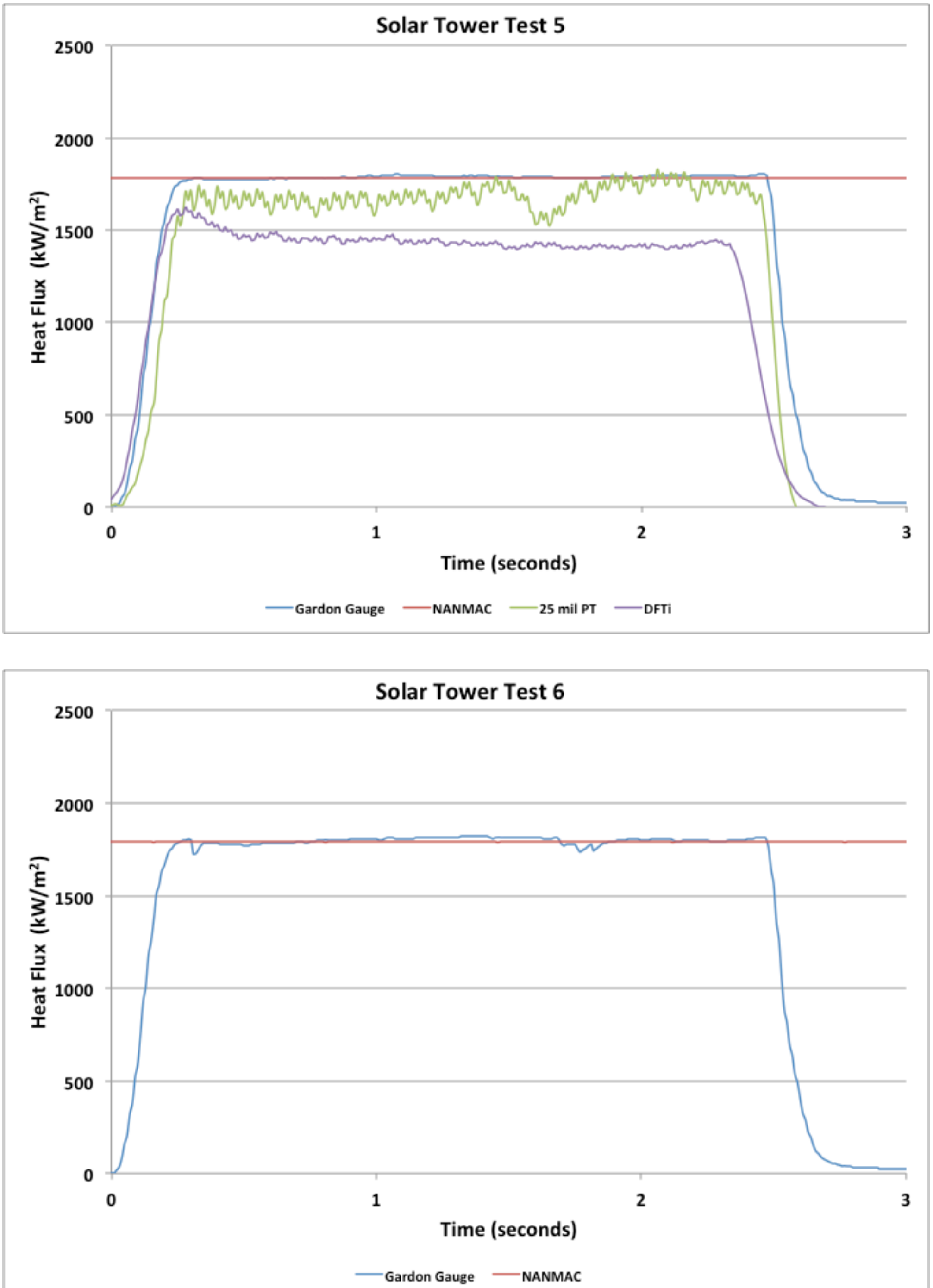

Figure 21. Heat flux estimates for Tests 5 and 6 (1.5 MW/m^2 nominal exposure)

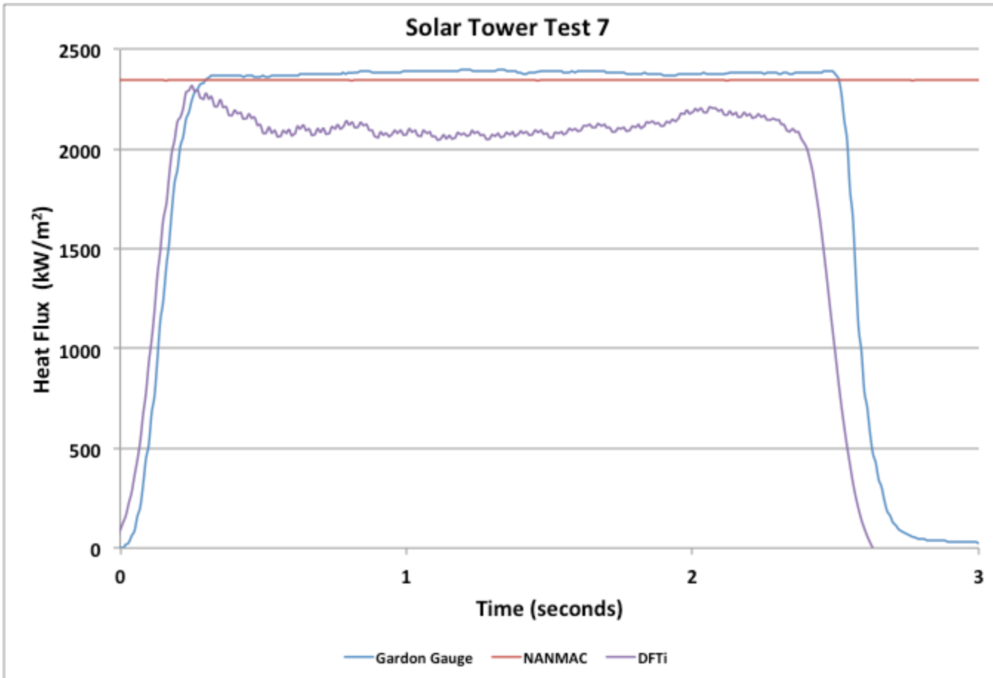

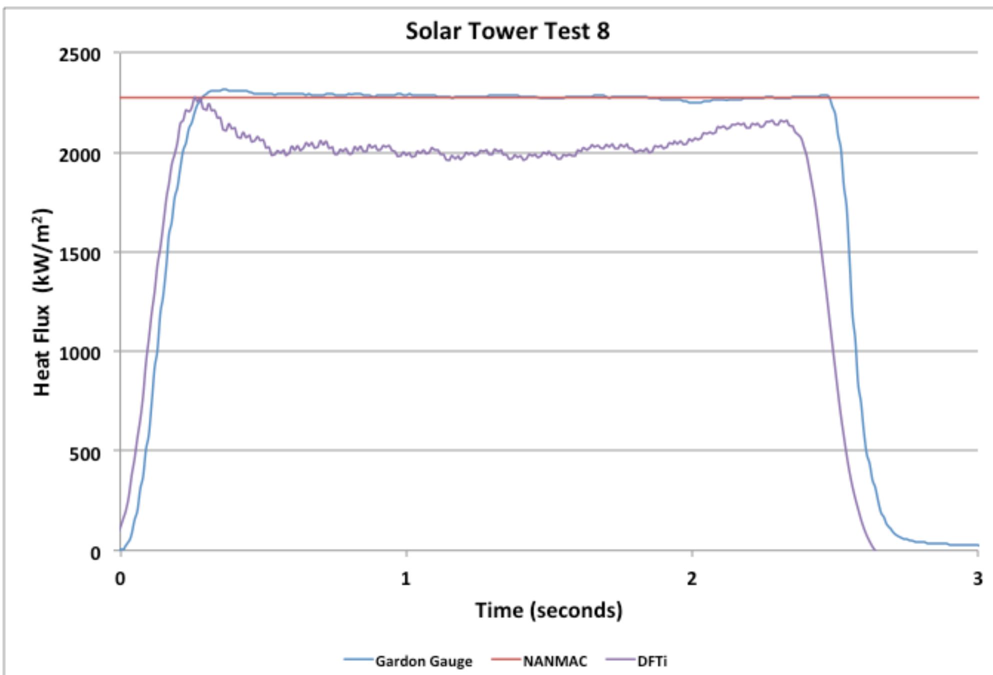

Figure 22. Heat flux estimates for Tests 7 and 8 (2 MW/m^2 nominal exposure)

Table 3. OMEGALAQ peak temperature readings

Test ID	Plate Thickness	OMEGALAQ - Range for Peak Temperature (ºC)	Peak Temperature Read by an Active Gauge [for reference] (ºC)
Test 2	18 mil	510-566	430 (Test 1 PT)
Test 4	18 mil	816-927	836 (Test 3 PT)
	25 mil	760-788	617 (Test 3 PT)
Test 6	65 mil	510-566	472 (Test 5 DFTi)
	25 mil	>1038	952 (Test 5 PT)
Test 8	65 mil	760-788	658 (Test 8 DFTi)

Thermoplastic and thermoset cable segments were used as part of this test series to obtain anecdotal heat damage information during Tests 2, 4, 6, and 7. Photos illustrating the exterior condition of the cables after they were exposed to the different heat levels are shown in Figure 23. In all these photos, the thermoset cable is positioned on the left and the thermoplastic is on the right. The information obtained from these exposures is very valuable because damage to real NPP targets can be observed and not inferred. Flames were also observed from the back of the instrumentation cluster during some tests. Figure 24 shows a close-up on the cable segments from Test 7. Note that flaking of the cable jacket occurred. This flaking appeared to be more pronounced on the thermoset.

A portion of the Bikini pressure gauge was also exposed to high heat flux after the core set of tests was completed. This extra test (Test 9) was performed with an arbitrary heat flux exposure, based on the available sunlight at the time of the test (1.84 MW/m^2). The intention of that exposure was to determine if it was possible to distinguish between pressure-sensing holes that were ruptured (or damaged) by overpressure versus by heat. To do this, one of the pressure-sensing holes of the Bikini gauge was ruptured by pressure. That hole and another (adjacent) pristine hole were then exposed to the high heat. Photos of the Bikini gauge before and after the test are shown in Figure 25. Note that only a portion of the whole Bikini gauge was exposed to the high heat and that is why the aluminum foil in the largest hole shows as only partially damaged. Aluminum foil is often used in fire testing to protect test equipment (by reflecting the incident energy), but the heat flux of this experiment was over twenty times larger than that observed in typical open pool fires. Thus, damage to the aluminum foil was expected.

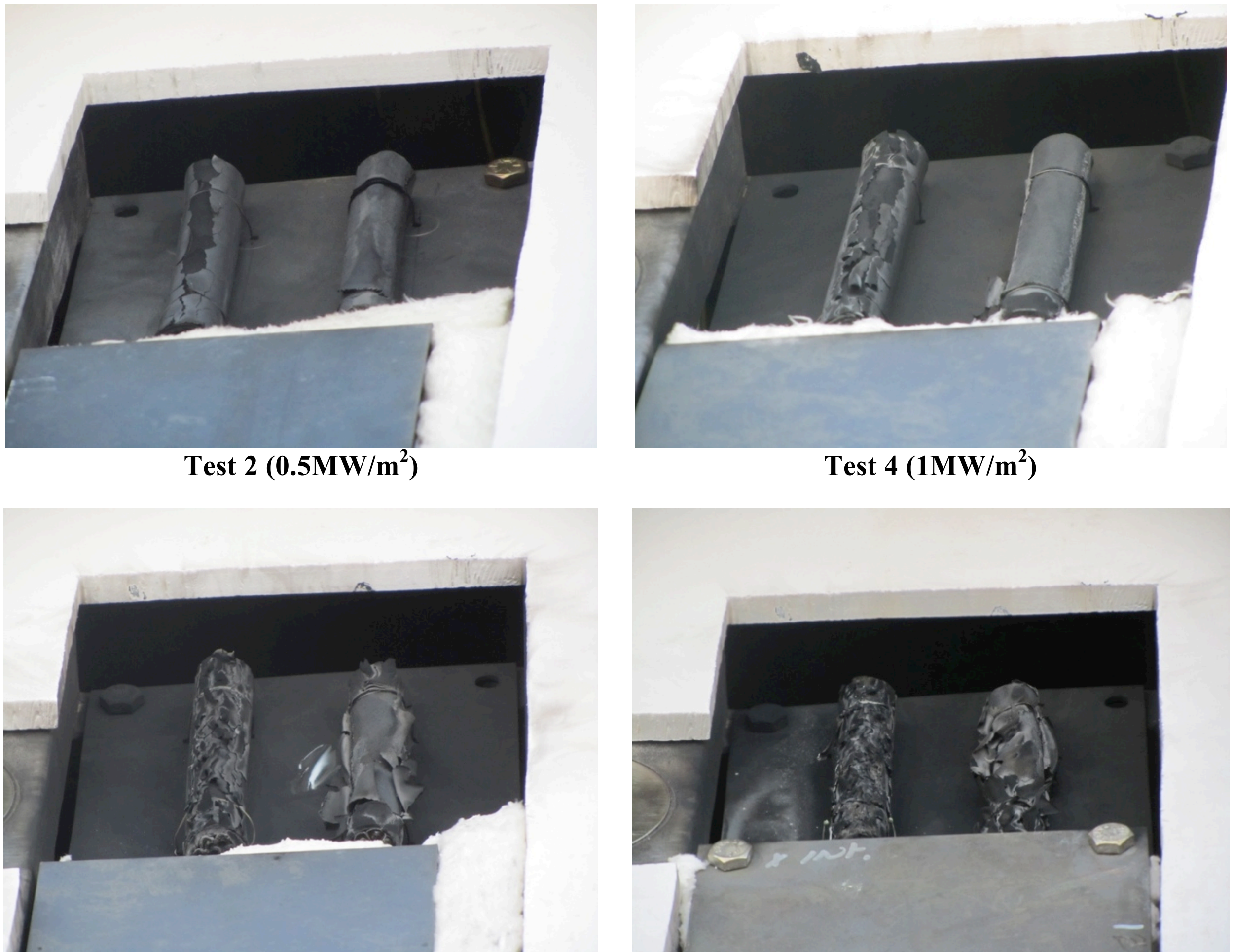

Test 2 (0.5MW/m^2) Test 4 (1MW/m^2)

Test 6 (1.5MW/m^2) Test 7 (2MW/m^2)

Figure 23. Physical damage to cable segments

Figure 24. Close-up of cable segments after Test 7 (thermoset left & thermoplastic right)

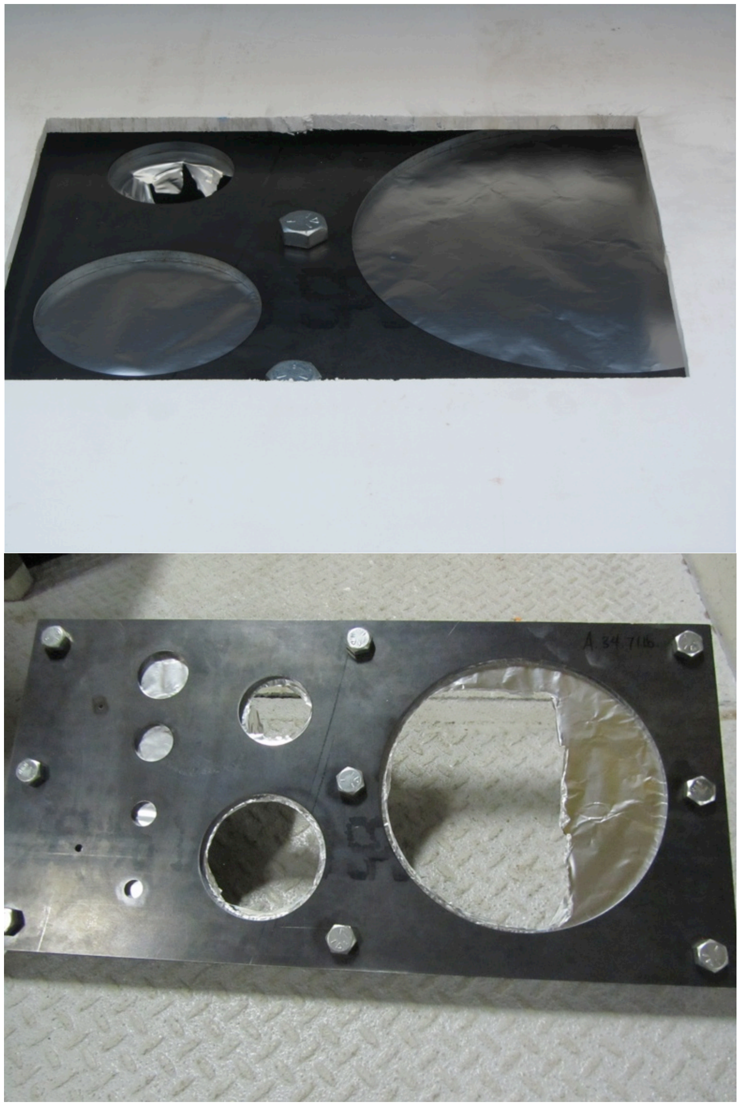

Figure 25. Bikini gauge before (top) and after (bottom) a high heat flux exposure

4 Blast Testing: Description and Summary of Results

It is known that electrical arcs on the order of 7.2 kV, 20 kA, and a few seconds in duration result in enormous temperatures near the fault and have resulted in measured pressure amplitudes of about 21 kPa (3 psi) at 1 m (3.3 ft) distances.[4] The simulated pressure tests presented here used bulk Composition C-4 high explosive (HE) to generate a pressure waveform meant to simulate the estimated peak pressures associated with HEAFs. These tests were performed at SNL’s Terminal Ballistic Facility (TBF). The SNL TBF can provide custom loadings using conventional explosives for projectile flight, terminal ballistics, armor performance, and fusing investigations.

For these tests, plate thermometers, plates with OMEGALAQ, cable segments, Bikini gauges, and pencil pressure gauges were used. Note that the instrumentation cluster frame shown earlier in this document (Figure 11) was not used during the blast tests. Instead metal stands were designed to hold the probes 1.2 m (4 ft) above ground. The objectives of the tests were to verify Bikini gauge peak pressures with pencil pressure gauges and examine the impact that a range of peak pressures has on pressure and temperature gauges and on cable segments.

4.1 Blast test set-up

Three sets of two stands with instrumentation were placed radially around the HE at 0.9, 1.8, and 2.7 m (3, 6, and 9 ft). One Bikini gauge and a piezoelectric pressure transducer were mounted on one of the stands of the set and a combination of a plate thermometer, a plate with OMEGALAQ, and thermoset and thermoplastic cable segments were mounted on the other stand of the set. The Bikini pressure gauges were constructed of two 0.6 by 33 by 66 cm (0.25 by 13 by 26 in) steel plates sandwiching a sheet of aluminum foil and held together with nine matching bolt holes, identical to those specified by Avery and Ball [5]. The aluminum foil used in the Bikini gauges was 0.254 mm (0.001 in or 1 mil). The piezoelectric pressure transducer mounted in a steel fixture held by one of the bolts of the Bikini gauges was used to attempt to nominally measure the reflected (normal as opposed to side-on) pressure wave form (see Figure 26). In addition, two pencil-type piezoelectric pressure gauges, mounted on tripods at 1.2 m (4 ft) height and placed at 0.9 and 1.8 m (3 and 6 ft) from the HE, measured the side-on overpressure to verify peak pressure readings at the two Bikini gauges closest to the HE. Instrumentation was arranged so that it did not obstruct the HE line-of-sight with other instrumentation (see Figure 26).

Testing took place at the TBF on the explosive firing pad revetment. The test matrix is shown in Table 4. The HE consisted of varying masses of Composition C-4, which was initiated on the surface with a Reynolds (RISI) RP-1 detonator and suspended at the instrumentation cluster height [1.2 m (4 ft)] off the ground using a string net. With the exception of Test Arc-01, the Composition C-4 HE was rolled into a sphere by hand resulting in a density of 0.58-0.6 g/cm^3. To compare the effect of shape and HE density on measured pressure, the HE for Test Arc-01 was pressed into a thin-walled cardboard cylinder with length-to-diameter ratio of about 1 using a plastic rod resulting in a density of 1.66 g/cm^3 (near the theoretical maximum density).

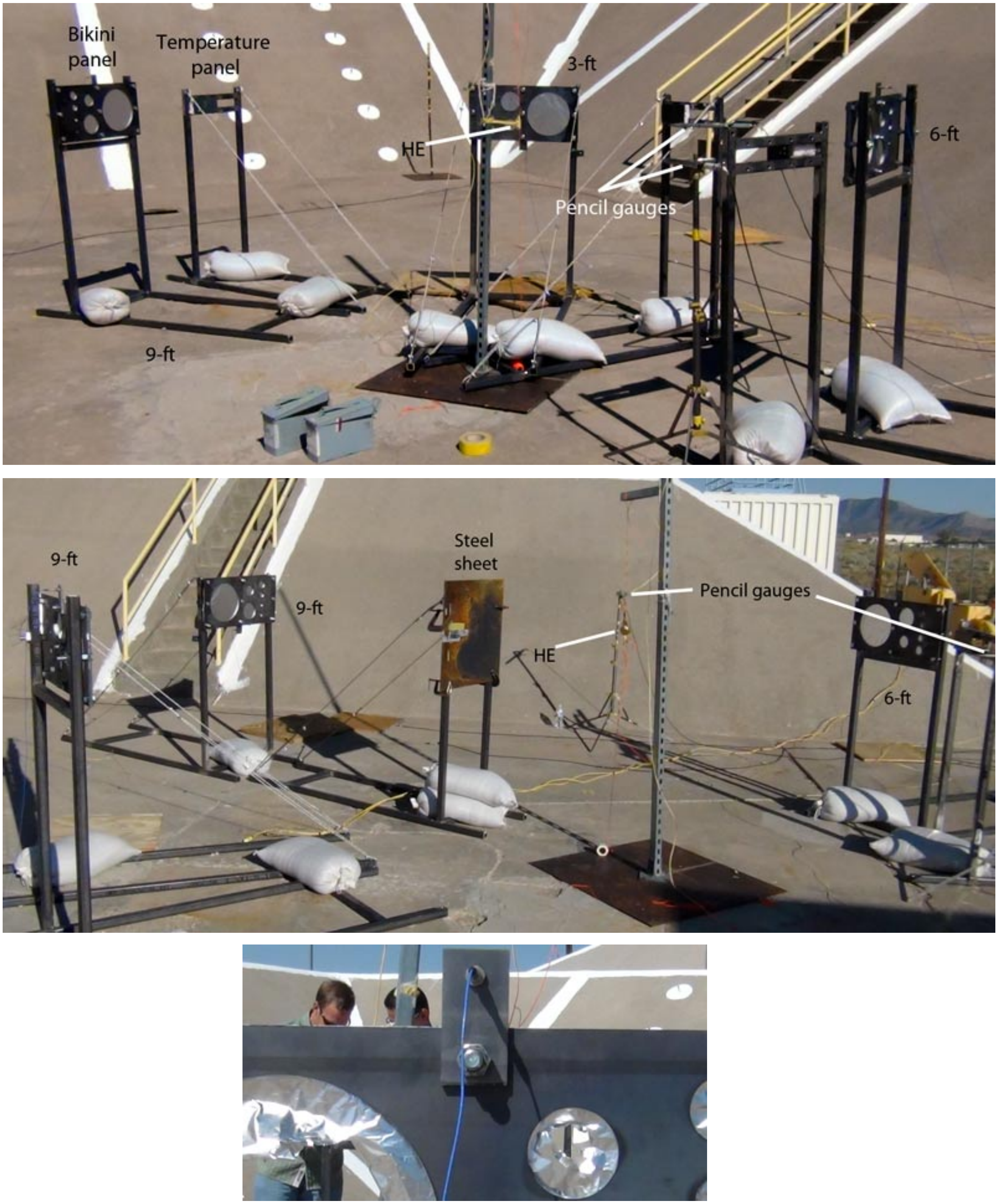

Figure 26. Set-up for Tests Arc-01 - 03 (top); Test Arc-04 (middle); reflected pressure gauge mounted on the Bikini gauge (bottom)

It is necessary to document and discuss a few exceptions to the test set-up. Test Arc-00 was a preliminary test performed with 20 g HE and only included a single Bikini gauge, placed 3 ft from the HE. Due to the extremely high heat flux expected during the actual electrical arcing tests, a method to shield the thin aluminum foil in the Bikini gauge was examined during Test Arc-04. For the 100 g Arc-04 test, a thin 0.6 by 0.6 m (2 by 2 ft) sheet of steel 1.6 mm (1/16 in) thick was placed between the HE and the Bikini gauge [0.91 m (3 ft) from the HE and 1.8 m (6 ft) from the Bikini gauge]. For comparison, a second Bikini gauge was placed in line of sight of the HE, 2.7 m (9 ft) away. The third Bikini gauge was positioned 1.8 m (6 ft) from the HE (see Figure 26).

In addition to pressure data, two high-speed cameras recorded video of the rupture of the Bikini gauges and a high definition real time camera (30 frames per second) recorded video for each test. Time of arrival (TOA) and peak pressure of the shock was predicted for each test using the DDESB Blast Effects Computer [6] accounting for height above sea level. Predictions are given in Table 4. These predictions were used as reference for the selection of pressure transducers. Pressure data was recorded with a Tektronix Model DPO 7104 digitizer using pressure transducers made by PCB Piezotronics, Inc. Details on the instrumentation used can be found in Appendix B.

Table 4. Test matrix with estimated peak pressure for each test

Test ID	Test Date	Mass C-4 (g)	Cluster 1 @ 0.91 m (3 ft)		Cluster 2 @ 1.82 m (6 ft)		Cluster 3 @ 2.74 m (9 ft)	
			Side-on Pressure (psi)*	TOA (ms)	Side-on Pressure (psi)*	TOA (ms)	Side-on Pressure (psi)*	TOA (ms)
Arc-00	9/28/12	20	14.95	1.02	----	----	----	----
Arc-01	10/4/12	20	14.95	1.02	4.0	3.15	2.2	5.53
Arc-02	10/4/12	10	9.3	1.21	2.8	3.5	1.57	5.9
Arc-03	10/4/12	5	6.0	1.40	2.0	3.75	1.16	6.22
Arc-04	10/4/12	100	----	----	10.8	2.30	5.03	4.42

* 1 psi = 6.895 kPa

4.2 Blast test results and discussion

The Bikini gauges indicate the peak pressure measured by the number of holes ruptured. The gauge design was calibrated by Avery and Ball [6] with piezoelectric pressure gauges during a test series at China Lake using 14.3 kg of Pentolite HE. Avery and Ball considered a rupture to be “only those holes in which several tears in the aluminum foil extend[ed] the entire diameter of the hole.” The calibration results are shown in Table 5.

Table 5. Bikini Gauge Calibration[6]

Hole #	Hole Diameter (in)*	Minimum Pressure to Rupture (psi)**
1	10	0.95
2	4.5	1.9
3	2.75	2.8
4	2	3.7
5	1.5	4.6
6	15/16	6.9
7	43/64	9.1
8	19/64	18.0
9	11/64	28.0

* 1 in = 2.54 cm; ** 1 psi = 6.895 kPa

Results from the five tests performed at the TBF (Arc-01 to 05) are summarized in Table 6. This table gives the peak shock side-on overpressure and time of arrival measured by the two pencil pressure gauges, the number of holes ruptured in the Bikini aluminum foil pressure panels, and the estimated peak pressure measured by the Bikini gauges (by using the calibration in Table 5). The interpretation of hole-rupture turned out to be very significant. For most tests there were varying degrees of punctures on 4 to 7 of the Bikini gauges holes (from pin holes to complete foil displacement). Appendix C shows photos of the back side of every Bikini gauge tested. Appendix D shows the pressure history of the pencil gauges, from which the peak pressure (in psi) and TOA (in ms) data shown in Table 6 were ascertained. Note that the response at time zero shown on each of the pressure history plots in Appendix D is a fiducial marker used as reference to estimate TOA.

The repeated 20 g HE tests, Arc-00 (spherical) and Arc-01 (cylindrical) were in good agreement at 0.9 m (3 ft) for overpressure and TOA, showing more variation in overpressure at 1.82 m (6 ft). Because of the similarity between these two tests, the remaining three tests were performed with spherical (0.58-0.6 g/cm^3) HE.

The results in Table 6 show good agreement at 0.9 m (3 ft) with the Bikini gauge pressure range enveloping all pencil-gauge measured peak pressures. At 1.8 and 2.7 m (6 and 9 ft) there was less agreement between the Bikini gauges and the pencil gauges. At these distances, the Bikini gauges measured both higher and lower pressures relative to the pencil pressure data. For the four instances (Arc-01 at 6-ft, Arc-03 at 6-ft and Arc-04 at 6- and 9-ft) where the Bikini pressure range did not envelope the pressure measured by the pencil gauge, the Bikini pressure range averaged a 21% deviation from the pencil gauge readings. However, this deviation was largely biased by the Arc-03 1.8 m (6 ft) Bikini gauge, which, although it showed a large tear on the largest hole, was not deemed a rupture. In all, the Bikini pressure range deviated 9% from the pencil gauge readings (the reference) [5%, if Arc-03 1.8 m (6 ft) had a rupture of its largest hole].

Table 6. Blast test results

Distance from HE	Measured Parameter	Test ID				
		Arc-00 (20g HE)	Arc-01 (20g HE)	Arc-02 (10g HE)	Arc-03 (5g HE)	Arc-04 (100g HE)
0.91 m (3 ft)	Pencil Gauge Peak Pressure (psi)*	9.051	9.009	5.411	4.426	----
	TOA (ms)	1.131	1.071	1.307	1.442	----
	Holes Ruptured	6	6	5	4	----
	Bikini Pressure Range (psi)*	6.9-9.1	6.9-9.1	4.6-6.9	3.7-4.6	----
	% Deviation (Bikini)	0%	0%	0%	0%	----
1.82 m (6 ft)	Pencil Gauge Peak Pressure (psi)*	1.612	2.741	2.128	1.591	7.067
	TOA (ms)	3.338	3.249	3.566	3.796	2.5
	Holes Ruptured	----	3	2	0	7
	Bikini Pressure Range (psi)*	----	2.8-3.7	1.9-2.8	<0.95	9.1-18.0
	% Deviation (Bikini)	----	2%	0%	>40%	29%
2.74 m (9 ft)	Pencil Gauge Peak Pressure (psi)*	----	----	----	----	3.312
	TOA (ms)	----	----	----	----	4.737
	Holes Ruptured	----	0	0	0	4
	Bikini Pressure Range (psi)*	----	<0.95	<0.95	<0.95	3.7-4.6
	% Deviation (Bikini)	----	----	----	----	12%
2.74 m (9 ft) Shielded	Holes Ruptured	----	----	----	----	5
	Bikini Pressure Range (psi)*	----	----	----	----	4.6-6.9

* 1 psi = 6.895 kPa

Prior to testing, the reflected (normal) pressure was predicted (with the DDESB calculator) to be greater than twice the side-on pressure, but consistently measured considerably lower (see Appendix E).

For Arc-04, both Bikini gauges (unshielded and shielded) at 9-ft recorded higher pressures than the unshielded pencil gauge with the shielded Bikini gauge indicating the highest peak pressure. Because pressure effects can be differentiated from the effects of high heat flux, as demonstrated during the Solar Tower Test 9, shielding the Bikini gauge may not be necessary.

Data from the plate thermometers was recorded during the tests despite damage to one of them by fragments from the blast as shown in Figure 27. However, the measured temperatures were indistinguishable from ambient. Therefore, temperature results are not presented in this document. There was little effect on the OMEGALAQ that was applied on some of the thin metal plates. That is, the lacquers stayed on the plates (very little flaking caused by the shockwave was observed). Like the plate thermometers, the lacquers did not record any temperature increase. As a final note, the thermoset and thermoplastic cable samples that were mounted on the stands did not show any sign of damage or degradation due to the exposure to the blasts.

Figure 27. Damage to a plate thermometer during Test Arc-01

5 Lessons Learned, Conclusions, and Recommendations

Probes that can be used to take heat and pressure measurements from HEAF testing were identified and tested as part of this test program. The objective was to determine which probes are better suited to take the necessary measurement during future HEAF testing to advance the state of the art method for quantifying nuclear power plant fire risk from HEAF events. This objective was met, as instrumentation to obtain pressure, temperature, and emissive power resulting from HEAF testing were identified. Both passive and active gauges performed well and can be used to estimate temperature, heat flux, and pressure from these types of events. Fast-response DFTs, plate thermometers, heat flux gauges, and pressure gauges are necessary to collect the desired data.

The following nine observations and conclusions can be made from the high heat flux tests. The first three bullets refer to measurement techniques that did not work as required for HEAF testing applications. The next five bullets refer to instruments that performed adequately for use in future HEAF testing. The last bullet contains comments on the ability to read recorded pressures by the passive pressure gauge even after it has been exposed to a high heat flux environment.

- Probes that were instrumented with sheathed thermocouples had unacceptable slow response times for use in HEAF testing. Those types of probes are more appropriately suited for longer duration events.
- The slow sampling rate permitted by the software provided by the manufacturer of the IR sensor rendered the IR temperature readings unusable for the proper estimation of heat flux. It may be possible to read temperatures at faster rates if the probe is connected to a different data logger; this may be explored for future testing. However, this probe exhibited high sensitivity to radio frequencies (RF), as much noise was introduced into the readings when 2-way radios were used near the probe when performing the tests described in this document. Since RFs are produced during HEAF events, such sensitivity to RF can be a factor that renders this probe unusable for HEAF testing.
- Temperature-indicating lacquers provided a general idea for the peak temperatures of objects on which they were applied despite the rapid heating profiles used in these tests. However, temperature readings were only consistent with the active measurements in one test.
- Plate thermometers and DFTs instrumented with intrinsic Type K thermocouples were capable of responding adequately to the step change heat flux exposure. However, thermal losses by radiation and convection heat transfer increased the uncertainty in the incident heat flux estimates that were based on the readings from these probes.
- Plate thermometers and DFTs are very rugged and relatively inexpensive to fabricate. Physical damage caused by fragments that may come from an arc blast is not likely to affect the readings from these probes.
- The heat flux readings by the Gardon gauge were used as reference for "calibrating" the other gauges used in this test series. While a Gardon gauge is more difficult to setup (needs cooling and protection) than a plate thermometer, a DFT, or a NANMAC assembly, it is still a probe that could be considered as part of the instrumentation cluster used for future HEAF testing.
- The NANMAC thermocouple mounted on a stainless steel disk provided readings that were very consistent with the readings from the Gardon gauge for a constant heat flux environment. Development of a model for transient heat flux estimates using this temperature probe was not a part of this effort.
- The high heat fluxes applied to the thermoset and the thermoplastic cable segments resulted in appreciable physical cable damage, but little can be concluded on ignition point, and cable electrical functionality.
- It was possible to identify a previously ruptured disk even after the Bikini gauge was exposed to a very high heat flux. This was possible because the aluminum near the edge of the hole was maintained below its melting temperature due to the cooling provided by the thick metal plates that sandwich the aluminum foil to form the gauge. That is, the thick steel plates acted as a heat sink for the aluminum foil near the edge of the holes and the thin aluminum foil survived the 2 MW/m^2 exposure for 2.4 seconds.

The following observations and conclusions can be made from the blast tests:

- The Bikini gauges operated as designed, with read pressures deviating from the pressures measured by the pencil gauges by 5-9%, which was comparable to the results reported by Avery and Ball [5].

- The pressure transducers configured to estimate reflected pressures provided unexpectedly low pressure measurements. It would be best to expose the pressure transducer directly to the pressure pulse if one can find a way to protect the pressure-sensing surface of the gauge from the high incident heat flux coming off of a HEAF.
- The thermoset and thermoplastic cables segments did not exhibit any damage produced by the blast.

In summary, based on the lessons learned from this test series, it is recommended to use the Gardon gauge, the NANMAC, and intrinsic plate thermometers and DFTs to obtain the information needed during future HEAF testing to evaluate the current guidance on analyzing HEAF. Cable samples should also be used in future testing to obtain true anecdotal evidence of damage on real targets. Pressure should be measured with an active gauge if possible, but new ways of measuring reflected pressure while protecting the pressure transducer need to be considered. Passive temperature lacquers and Bikini gauges could be used as "backup" to active gauges, as they are inexpensive, easy to setup, and may provide an estimate of peak temperatures and pressures during testing. Active probes that are minimally affected by the high energies associated with HEAFs should be considered for use in future testing.

6 References

[1] Beck, J.V., B. Blackwell, and C.R. St. Clair, Jr., Inverse Heat Conduction: Ill-posed Problems, John Wiley & Sons, Inc., 1985.
[2] Beck, J.V., "*User's Manual for IHCP1D*, Program for Calculating Surface Heat Fluxes from Transient Temperatures Inside Solids," Version 8.0, Beck Engineering Consultants Company, Okemos, Michigan, January 12, 2010.
[3] Incropera, F.P., and D.P. DeWitt, Fundamentals of Heat and Mass Transfer, 4th ed., John Wiley & Sons, Inc., 1996. pp. 236-242.
[4] Lee, R.H., *Pressures Developed by Arcs*, IEEE Transactions on Industry Applications, Vol. 1A-23 No. 4, July/August 1987.
[5] Avery, A.M. and C.H. Ball, Test Report for Calibration of "Bikini" Blast Overpressure Gages, Naval Air Warfare Center Weapons Division, China Lake, CA, NAWCWPNS TM 7795, June 1995.
[6] Swisdak, M.M., Jr., J.M Ward, "Department of Defense Explosive Safety Board Blast Effects Computer User's Manual and Documentation," DDESB TP 17, May 2003.

Appendix A. Thermophysical Properties Used in IHCP

Thermophysical Properties of Inconel 600

Temperature (ºC)	Thermal Conductivity (W/m-ºC)	Volumetric Heat Capacity (J/m^3-ºC)
20	10.2	3930161
200	13.4	3946353
300	15.2	3963873
400	17	4018172
500	18.8	4191161
600	20.6	4576879
700	22.4	4967482
800	24.2	5118395
900	26	5149256
1000	27.8	5171504
1100	29.6	5216778
1200	31.4	5291101
1300	33.2	5396239
1400	35	5535099

Thermophysical Properties of Cerablanket (Density = 128 kg/m^3 or 8 lbs/ft^3)

Temperature (ºC)	Thermal Conductivity (W/m-ºC)		Temperature (ºC)	Volumetric Heat Capacity (J/m^3-ºC)
20.3	0.034		0	134500
22.1	0.0342		100	141018
26.5	0.0345		200	147163
28.3	0.0348		300	152937
30.1	0.0349		400	158338
141	0.0463		500	163368
232.4	0.0581		600	168025
330.3	0.0737		700	172311
505.7	0.1096		800	176224
537.5	0.1174		900	179765
645.2	0.1468		1000	182935
750.7	0.181		1100	185732
773.5	0.189		1200	188158
904.6	0.2405		1384	191648
1034.6	0.3012			
1384	0.4857			

Appendix B. Pressure Instrumentation

<u>Digitizers</u>

Manufacturer:	Tektronix
Model:	DPO 7104

Reflected Pressure Digitizer	SNL Asset #6567928	**Calibration Date**	1/25/2012
Free Field Pressure Pencils	SNL Asset #6562369	**Calibration Date**	11/18/2011
Thermocouple Data	SNL Asset #6562401	**Calibration Date**	1/25/2012

<u>Pressure Transducer Amplifiers</u>

Manufacturer:	PCB Piezotronics
Model:	482A16

<u>Reflected Pressure Gauges</u>

Manufacturer:	PCB Piezotronics
Model:	102A09 0-50 psi Flush Mount Gauge

3' Gauge	SNL Asset #48667	**Cal. Factor:**	493mV/psi	**Calibration Date**	10/1/2012
6' Gauge	SNL Asset #51026	**Cal. Factor:**	478mV/psi	**Calibration Date**	10/1/2012
9' Gauge	SNL Asset #48666	**Cal. Factor:**	503mV/psi	**Calibration Date**	10/1/2012

Note: 3' Reflected pressure gauge used as 9' shielded gauge on Arc-04 Test

<u>Free Field Pressure Pencils</u>

Manufacturer:	PCB Piezotronics
Model:	137A23 0-50 psi Pencil Gauge

3' Gauge	SNL Asset #48239	**Cal. Factor:**	129mV/psi	**Calibration Date**	9/17/2012
6' Gauge	SNL Asset #48237	**Cal. Factor:**	118mV/psi	**Calibration Date**	9/17/2012

<u>Thermocouples</u>

Manufacturer:	Omega
Model:	K-Type

Appendix C. Response of Bikini Gauges

Figure 28. Arc-00 Bikini Gauge Results for 3 ft

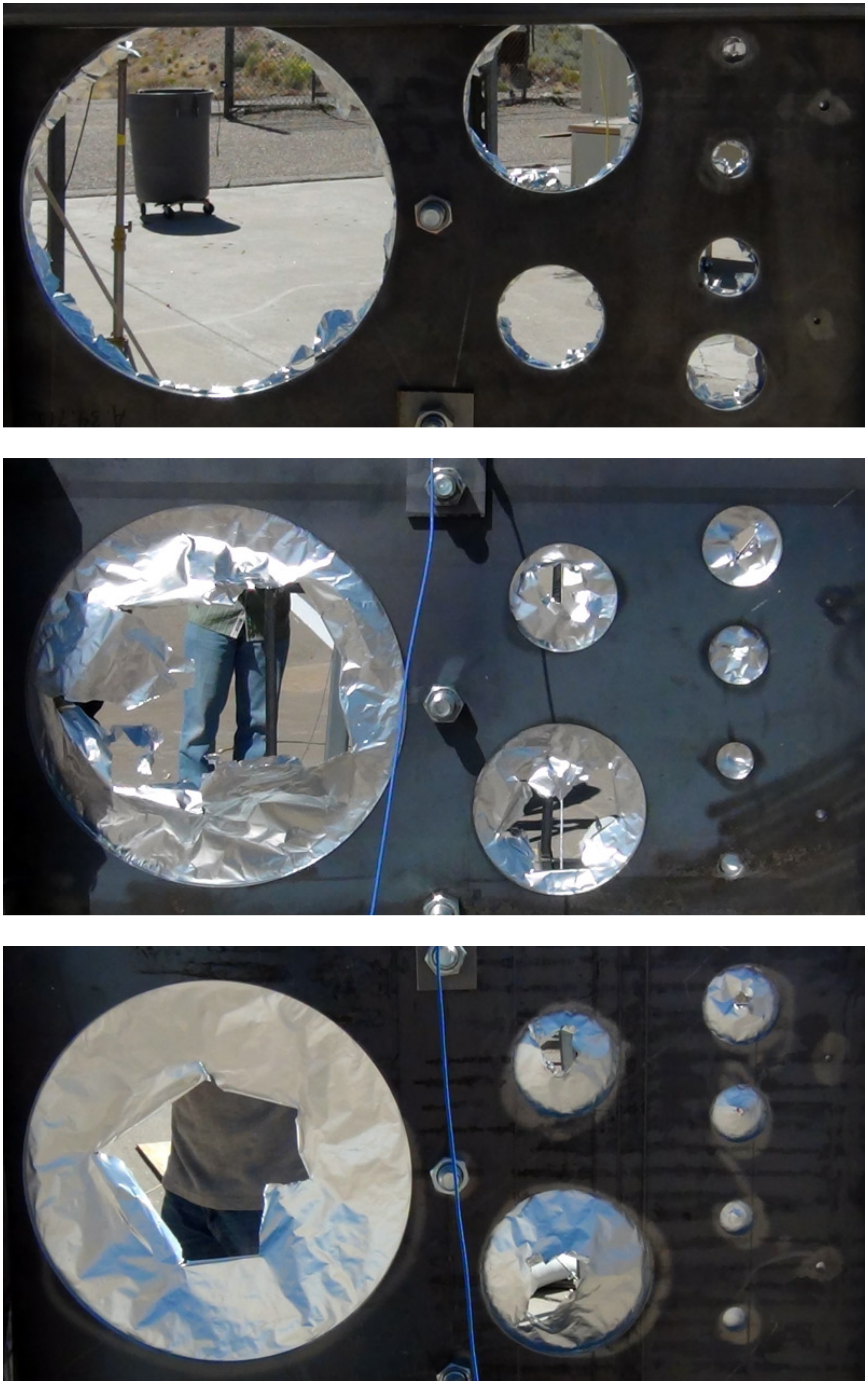

Figure 29. Arc-01 Bikini Gauge Results for 3 (top), 6 (middle), and 9 ft (bottom)

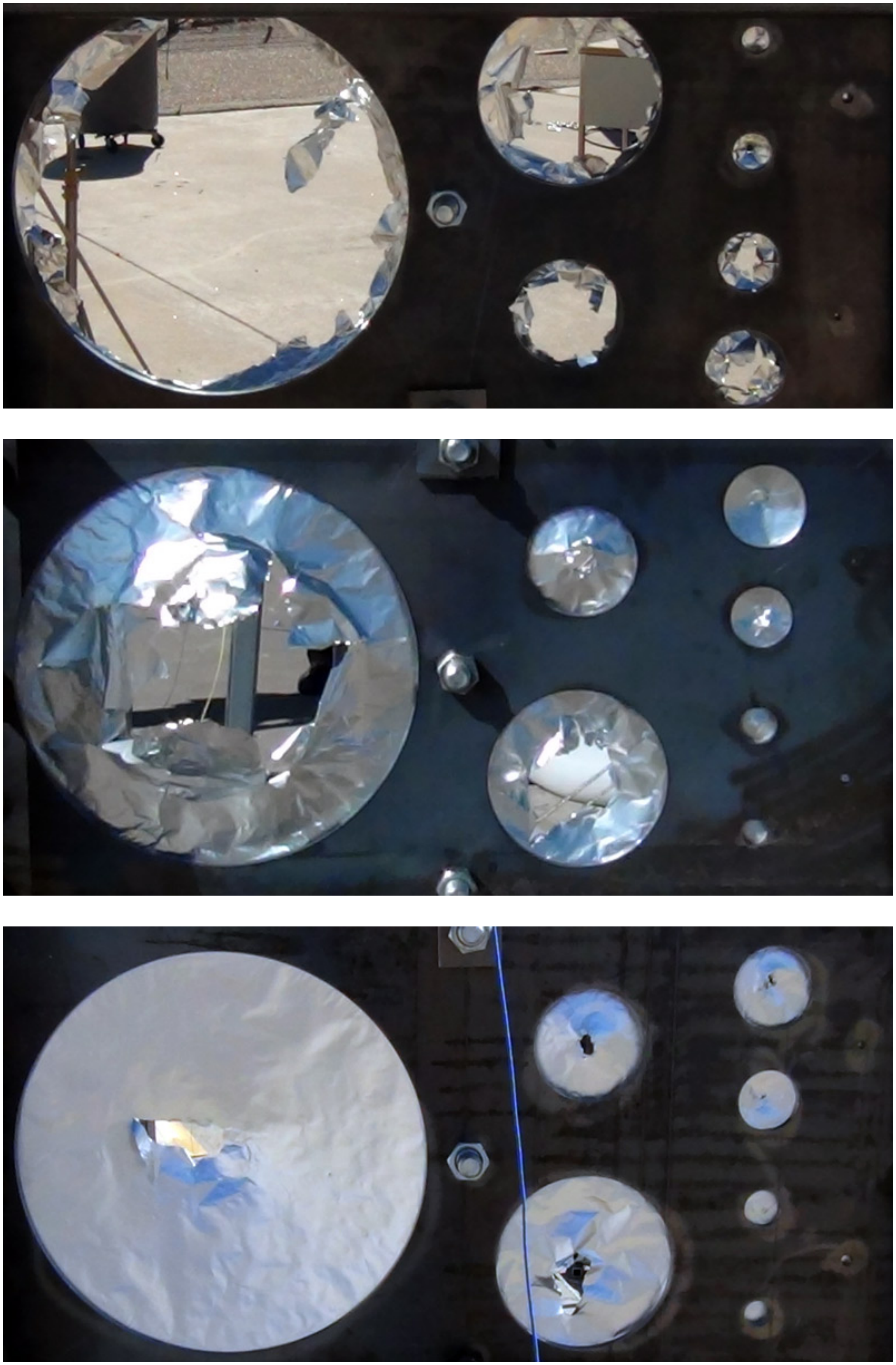

Figure 30. Arc-02 Bikini Gauge Results for 3 (top), 6 (middle), and 9 ft (bottom)

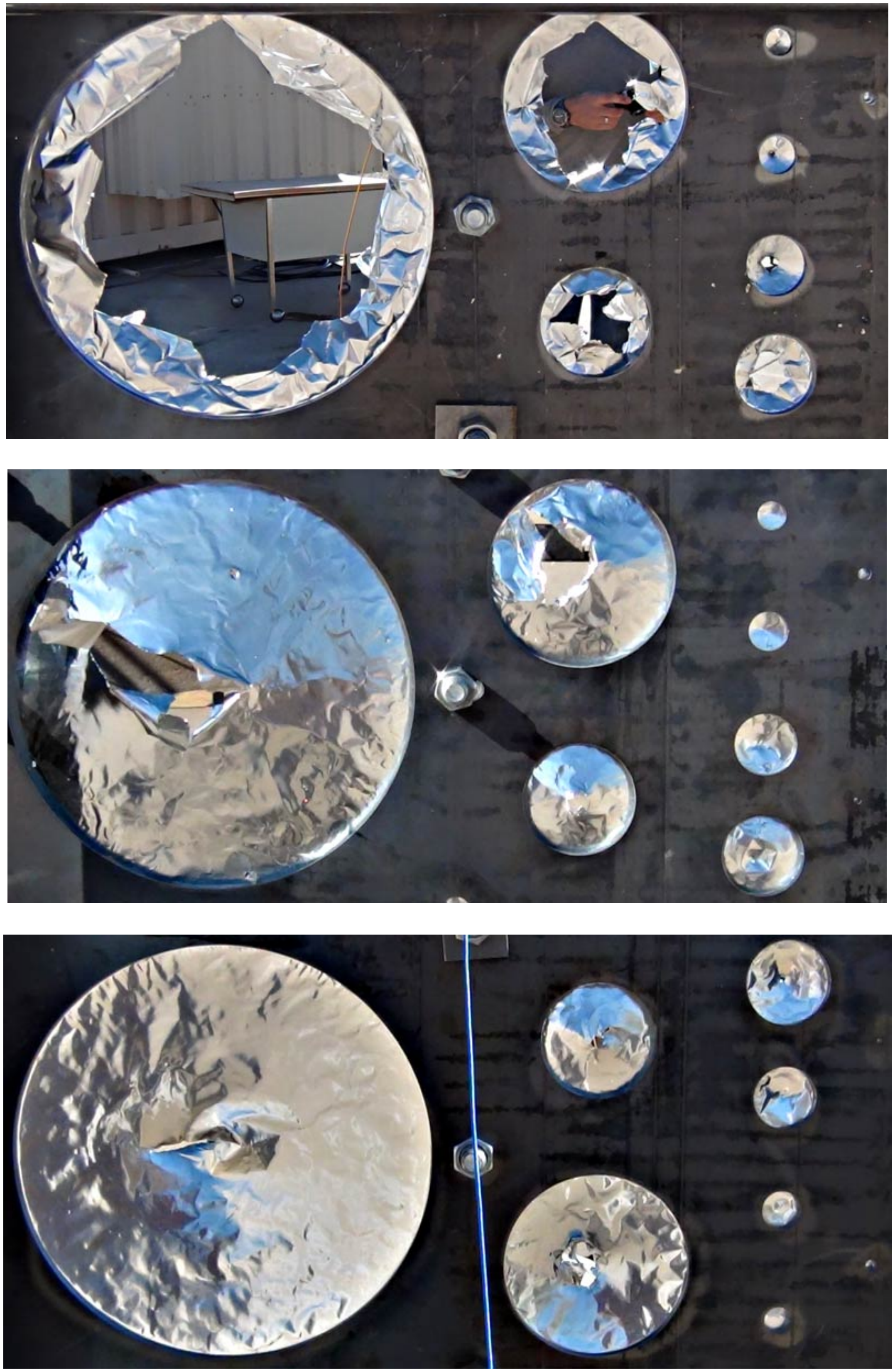

Figure 31. Arc-03 Bikini Gauge Results for 3 (top), 6 (middle), and 9 ft (bottom)

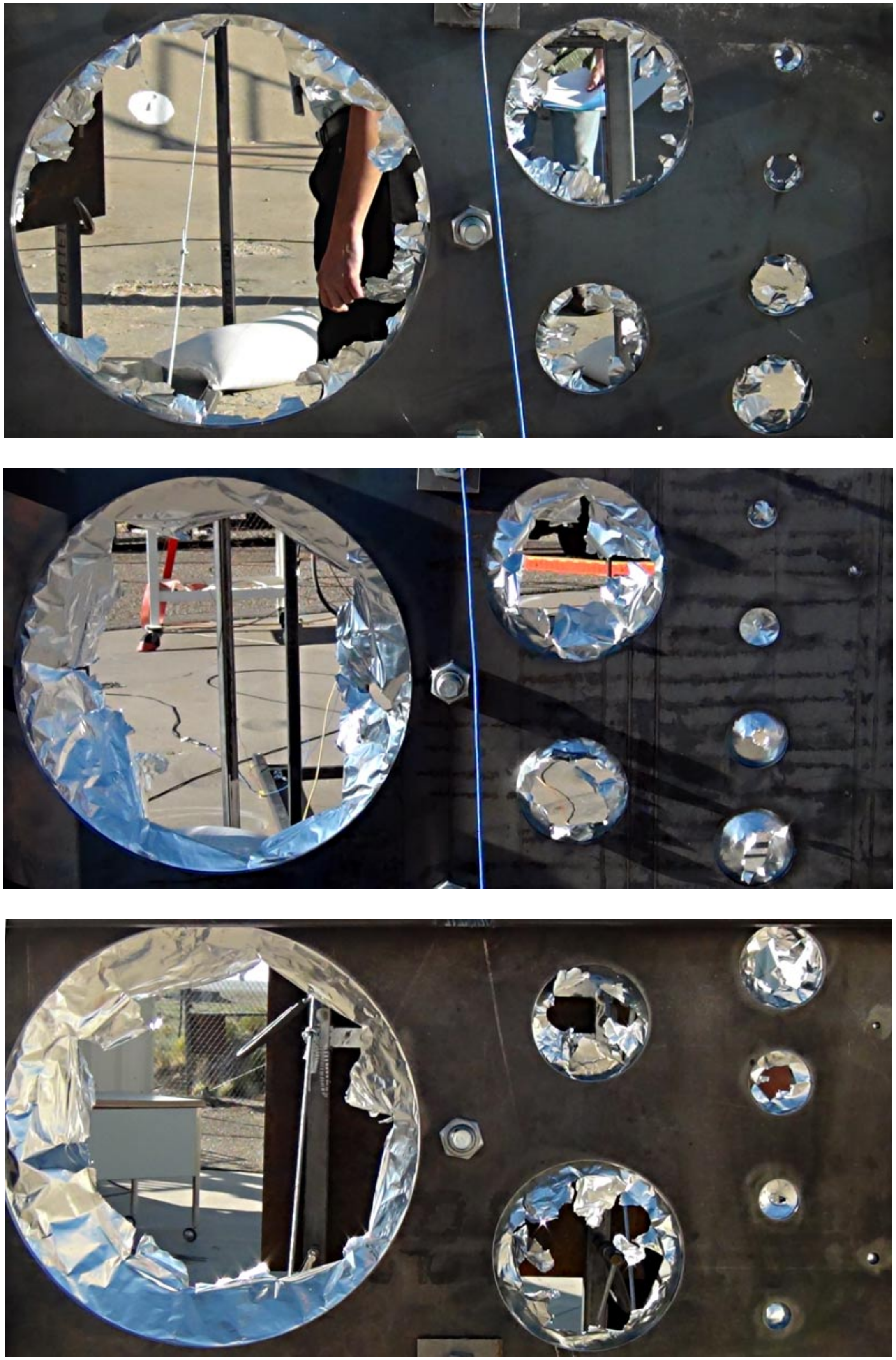

Figure 32. Arc-04 Bikini Gauge Results for 6 ft (top), 9 ft (middle), and 9 ft shielded (bottom)

Appendix D. Response of Pencil Gauges

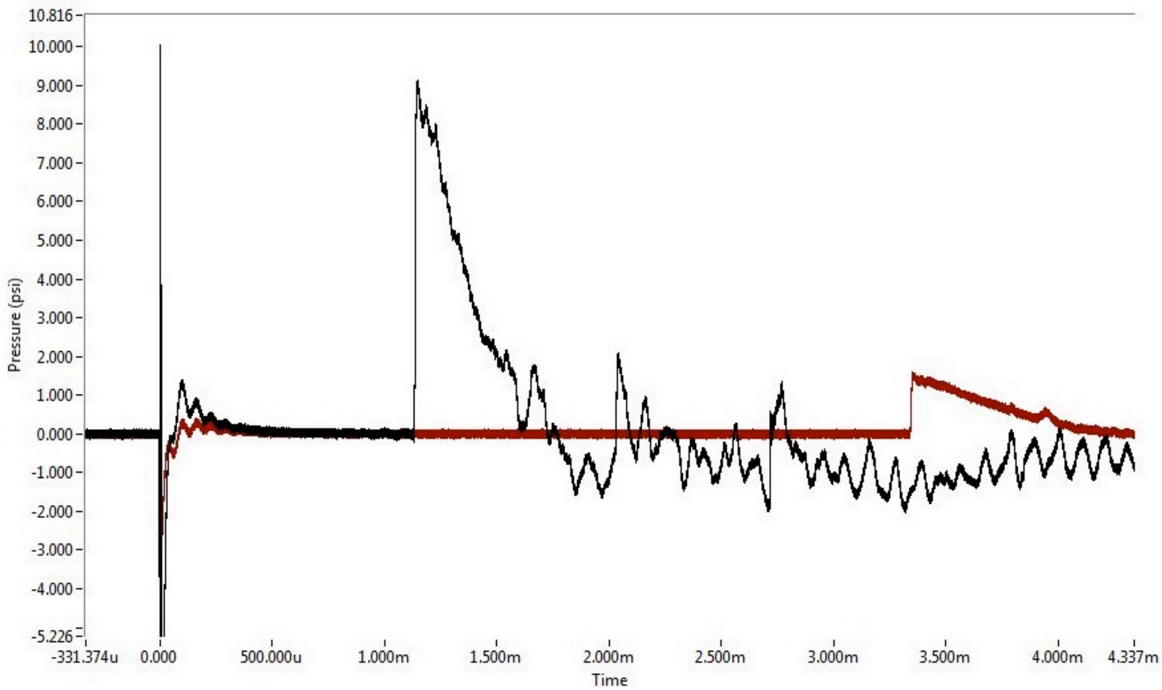

Figure 33. Arc-00 Pencil Gauge Pressure at 3 (black) and 6 ft (red). [Time in seconds]

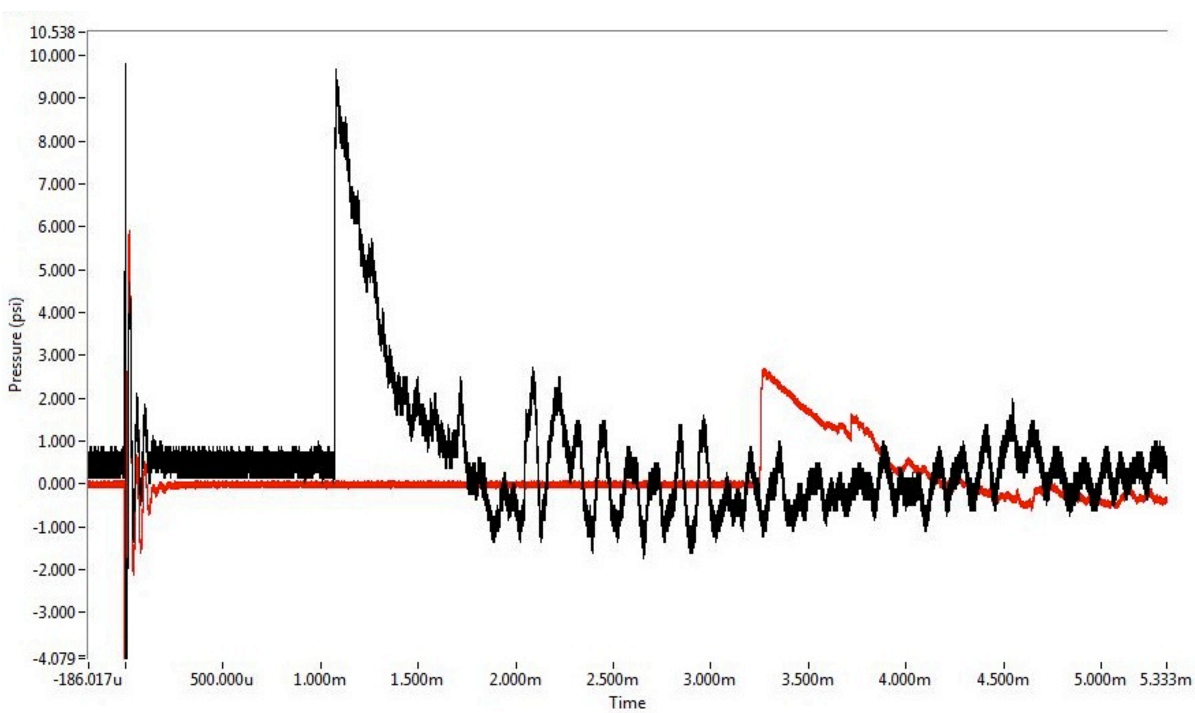

Figure 34. Arc-01 Pencil Gauge Pressure at 3 (black) and 6 ft (red). [Time in seconds]

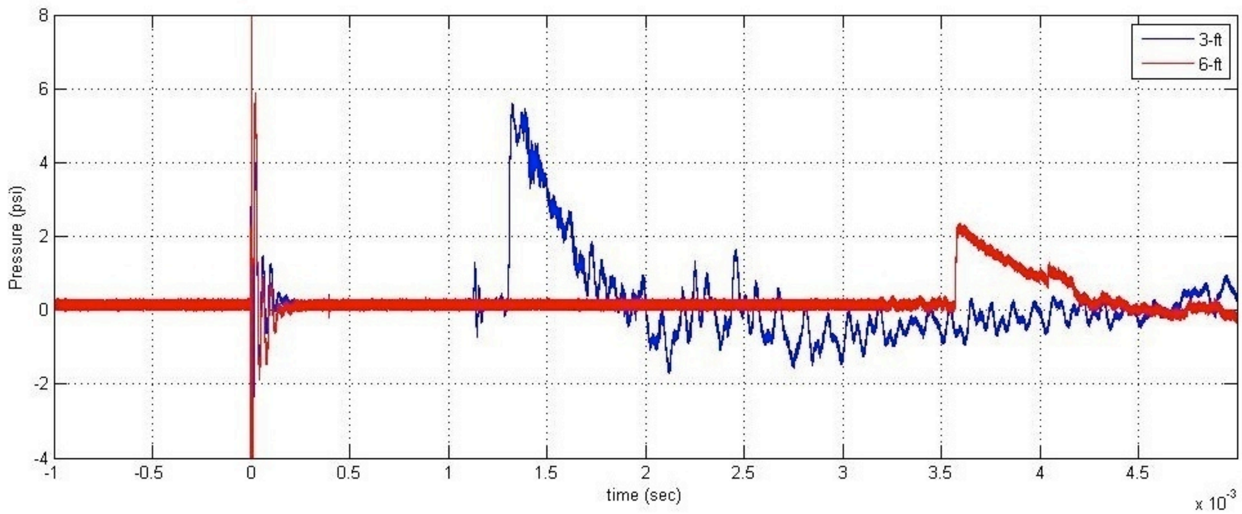

Figure 35. Arc-02 Pencil Gauge Pressure at 3 and 6 ft

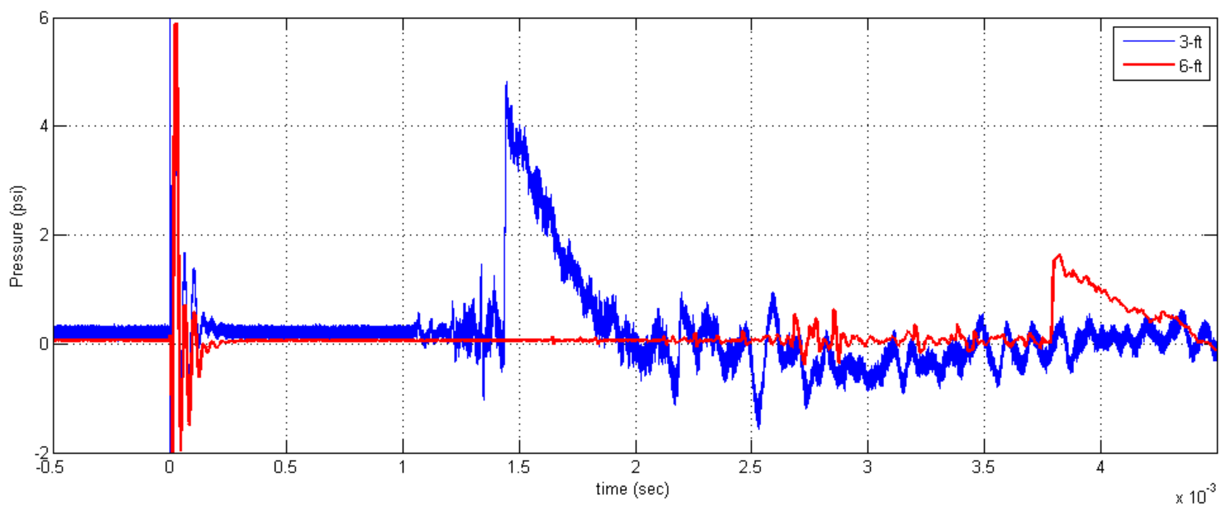

Figure 36. Arc-03 Pencil Gauge Pressure at 3 and 6 ft

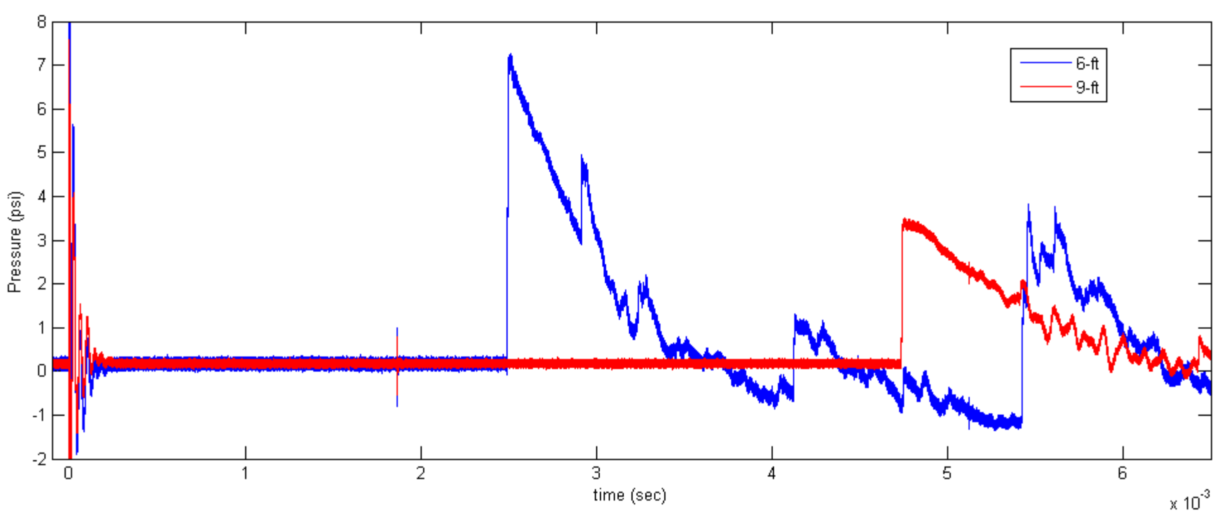

Figure 37. Arc-04 Pencil Gauge Pressure at 6 and 9 ft

Appendix E. Response of Pressure Gauges Used to Estimate Reflected Pressure

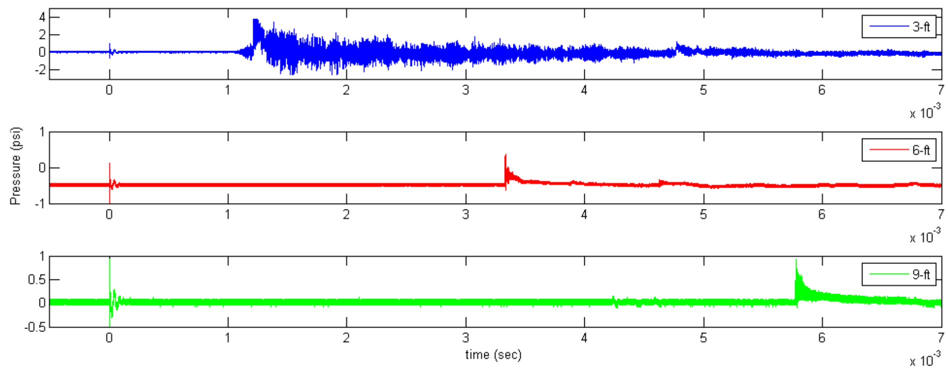

Figure 38. Arc-01 Reflected Pressure Gauges at 3, 6, and 9 ft

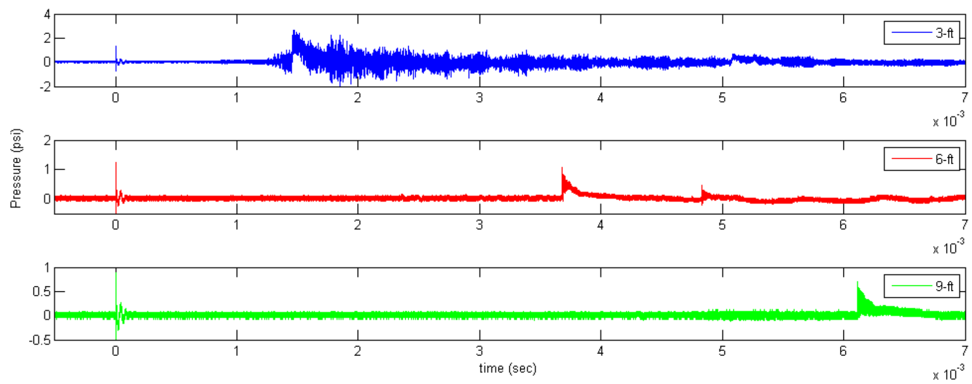

Figure 39. Arc-02 Reflected Pressure Gauges at 3, 6, and 9 ft

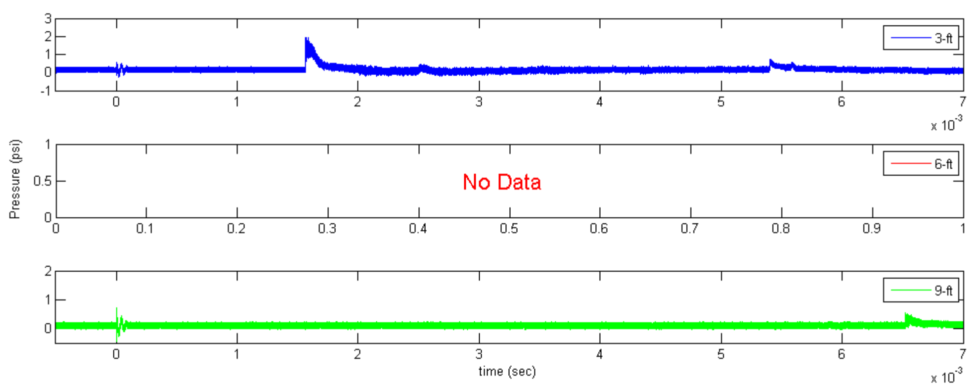

Figure 40. Arc-03 Reflected Pressure Gauges at 3, 6, and 9 ft

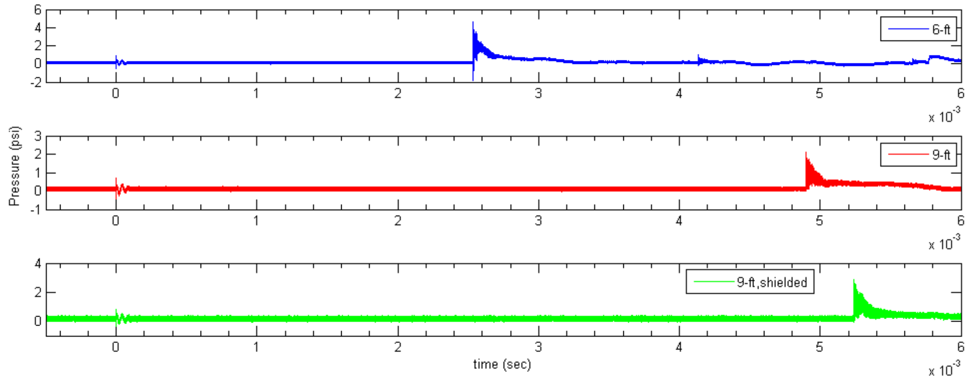

Figure 41. Arc-04 Reflected Pressure Gauges at 6 ft, 9 ft, and 9 ft shielded

Distribution

External (*electronic copy*)

1 Gabriel J. Taylor
U.S. Nuclear Regulatory Commission
Gabriel.Taylor@nrc.gov

Internal (*all electronic copy*)

1	MS0431	S. Burns	Org. 00263
1	MS0718	C. Lopez	Org. 06233
1	MS0718	V. Figueroa	Org. 06233
1	MS0744	P. Mattie	Org. 06233
1	MS0748	S. Nowlen	Org. 06231
1	MS1135	W. Gill	Org. 01532
1	MS1452	H. L. Stauffacher	Org. 02556
1	MS1454	W. Wente	Org. 02552

Technical Library (*electronic copy*)

1	MS0899	Technical Library	Org. 09536

Sandia National Laboratories